DS Journal of Artificial Intelligence and Robotics
Volume 4 Issue 2, 1-43, Apr - Jun 2026
ISSN: 2583-9926 / https://doi.org/10.59232/AIR-V4I2P101

Review Article

Basics Aspects to Identify Different Structures by Using Vibrational Spectroscopy Combined with the SQMFF Approach and Machine Learning

Silvia Antonia Brandán

Cátedra de Química General, Facultad de Bioquímica, Química y Farmacia, Universidad Nacional de Tucumán, Ayacucho 471, 4000, San Miguel de Tucumán, Tucumán, R. Argentina.

silvia.brandan@fbqf.unt.edu.ar

Received: 20 March 2026; Revised: 25 April 2026; Accepted: 18 May 2026; Published: 20 June 2026

Abstract - Vibrational assignments of some simple and complexes structures are analysed to know some basics aspects necessaries in the assignments of bands observed in the infrared and Raman spectra combined with the Scaled Quantum Mechanical Force Field (SQMFF) methodology. Fundamentals characteristics are necessaries in machine learning to replace a human expert in vibrational analysis. The use of that approach implies the correct definitions of normal internal coordinates of the different groups and rings present in the structures and, obviously, the knowledge of all vibration modes and, in particular, of regions where these groups are expected. The results show that it is possible to identify neutral and zwitterionic forms of L-phenylalanine from imidazolyl phenylalanine if the vibration modes of six- and five-member rings are performed. In chiral species, reliable assignments are performed when the R and S structures of enantiomers are optimized and analysed. However, in components of extract isolated from plants with a high number of atoms in the structures, only machine learning could replace a human expert due to the high computational cost involved in optimizations, studies of potential energy surfaces, and construction of internal coordinates. In species with multiple rings, the greatest difficulty lies in constructing the internal coordinates of different rings, while, in nitrate species, both coordination monodentate and bidentate modes of these groups should be considered in the assignments. In phosphate species, the correct use of a local C_{2v} or C_{3v} symmetry for the phosphate group is indispensable to assurance consistent and safe vibrational assignments. Finally, to identify hydrated species, the librations modes of water molecules, in addition to stretching and deformation modes, should also be identified and assigned.

Keywords - Molecular Structure; FTIR; DFT; SQMFF; Vibrational Assignments; Machine Learning.

1. Introduction

Advances in science and technology have enabled the rapid growth of computational chemistry and machine learning for multiple uses and applications; in particular, those related to vibrational spectroscopy and, for these reasons, only some more recent studies are mentioned in this work. [1-30] Thus, many models and methods have been developed for rapid predicting of infrared and Raman spectra as well as structure determination and functional group identification using various spectroscopies, among which vibrational spectroscopy stands out. [1, 5, 7, 8, 10, 12, 13, 15, 17-27]. The obvious reason is that this technique is one of the most regularly used to characterize structures with a small amount of sample in different aggregation states through the identification of its main

functional groups. [24,27,30] The use of this technique involves previous knowledge of the molecular structure, and the problem becomes more complicated when the sample is not crystalline and cannot be determined by using crystal X-ray diffraction. A problem common in the characterization of functional groups occurs when the structures of organic substances can present different conformations or configurations due to the presence of various dihedral angles and/or chiral carbon, when there is a mixture of isomers or enantiomers, or when the sample is an extract isolated from plants or an amino acid. [31] In these cases, the sample contains different species that present the same functional groups, but some of them change with the medium, as is the case with Amino Acids (AAs). [32-34] In the same way, the identifications of the different species and groups present in some clays or rare earths are also very difficult to identify because the different minerals present similar functional groups. [35] In addition, the use of mineral or vegetal carbon is a typical problem because it is impossible to identify the different organic and inorganic species present in these samples, including species containing different types of aromatic rings. [36] On the other side, the aliphatic and aromatic C-H stretching modes and those corresponding to N-H, NH_2, OH, CH_2, and CH_3 groups are expected in the same 4000-2800 cm^{-1} region, while among 1700 and 1500 cm^{-1} are expected C=C, C=N and N=N stretching and, in addition, deformation modes of OH and NH_2 groups. [37] Also, in the range of wavenumbers below 2000 $cm^{-1,}$ the presence of different four, five, six or more member rings and, of type of ring which can be fused or not (phenyl, pyridine, pyrazine, triazole, oxadiazole, indole, benzofuran, indazole, quinolone, benzotriazole) shows coupling of expected deformations and torsions of rings with other vibration modes. [37] Species identification by vibrational spectroscopy and the confirmation of a structure is only possible when all its expected vibration modes are fully assigned. It is impossible to confirm the structure of a newly synthesized compound with only a few bands observed in the spectra. In these cases, theoretical calculations are very helpful to confirm its structure. [37] In all cases, the medium is also very important in the structures, and it should be considered in the treatment of spectra in solution. [32-34] In general, the positions and intensities of bands attributed to vibration modes change with acceptor and donors of H-bond groups in the structures and, obviously, in solution. [32,33] Substances as bases and acids change with the pH of the medium. [32,33] Thus, an amino acid can be as neutral, containing NH_2 and COOH groups or, as a zwitterion in the solid phase or in solution, containing NH_3^+ and COO^- groups, which should be considered in a serious and rigorous vibrational study. [32-34] Then, the machine learning to characterize different structures should consider all multiple possibilities together with the normal internal coordinates that a human expert in vibrational analysis considers when a species should be completely identified by using the infrared and Raman spectra. [37] Hence, the aims of this work are to analyse simple and complexes structures of different species to know some basics aspects necessaries in the assignments of bands observed in the infrared and Raman spectra combined with the SQMFF methodology. Identification of simple and complicated structures containing different rings by using vibrational spectroscopy is essential for rigorous machine learning to be able to replace a human expert in vibrational analysis. Thus, machine learning should simplify the arduous task required to construct internal coordinates and to produce reliable and safe assignments taking into account the contributions of potential energy and, in particular, of species containing a high number of atoms. Hence, neutral and zwitterions of simple AAs and species isolated from plants, such as chiral and chalcone structures and also structures of alkaloids containing fused rings, such as the bicyclic (N-methyl-8a-zabicyclo [3.2.10]octane) group with a tertiary nitrogen atom, are analyzed in this work, also nitrate, phosphate and some hydrated species. Here, the vibrational studies of neutral and zwitterions of L-phenylalanine and imidazolyl phenylalanine AAs are reported for the first time in this work by using the SQMFF methodology. First, the confirmation of the structure of a species is the most important point to perform the assignments of all bands observed in the infrared and Raman spectra in the solid and/or liquid phases.

2. Computational Details

As was previously mentioned, the vibrational studies of neutral and zwitterions of L-phenylalanine and imidazolyl phenylalanine AAs are reported for the first time in this work by using the SQMFF methodology. The CIF file of L-phenylalanine (R1) corresponding to that experimental determined by X-ray diffraction by Mossou et

al. was considered as the initial structure. [33] Then, the structure of imidazolyl phenylalanine derivative (R2), taken from that similar to that reported by Ren et al. [27], was modelled by using the *GaussView* program. [39] After that, both neutral and zwitterionic structures of R1 and R2 were optimized in the gas phase (GP) and Aqueous Solution (AS) by using the hybrid B3LYP/6-311++G** method [40,41] with the Gaussian 16 program. [42] The harmonic force fields are calculated with the SQMFF procedure and the Molvib program [43-45] while the vibrational assignments were performed using Potential Energy Distribution (PED) and assignments for similar species. [34,37,46] Neutral and zwitterionic structures of R1 and R2 are shown in Figure 1. Only differences between the structures are the six- and five-member rings. Then, the structures and vibrational studies of 2',4'-dihydroxychalcone isolated from *Zuccagnia punctata* Cav. (Fabaceae) medicinal plant, tropane alkaloid scopolamine, camphor, acetogenins squamocin and motrilin, sesquiterpene lactone paradiolide, chromyl, niobyl p-xylylenediaminiumbis(nitrate), 1,3-Benzenedimethanaminium bis(trioxonitrate) and 1-buthyl-3-methyl imidazolium nitrate, 4-phenylpiperazine-1-ium dihydrogen phosphate and di-hydrated tetraphenylphosphonium chloride salt were already published. Hence, the corresponding structural and vibrational assignments are presented as supporting material.

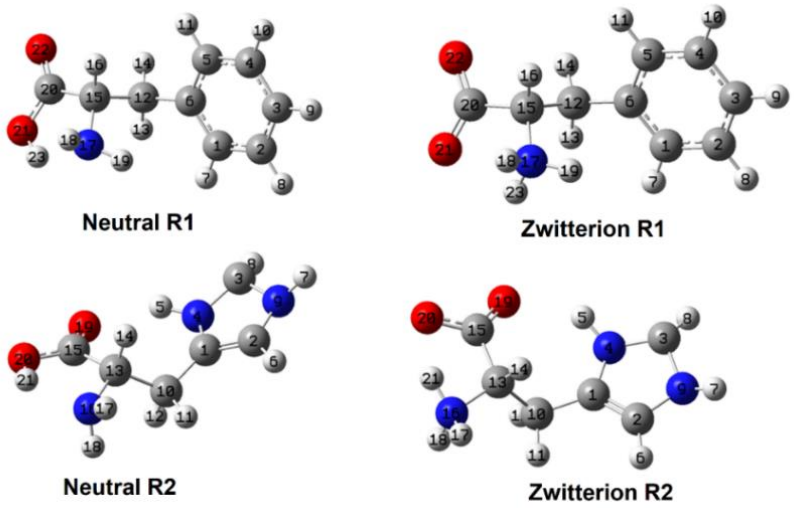

Fig. 1 Theoretical neutral and zwitterionic structures of R1 and R2 with the atom numbering.

3. Results and Discussion

3.1. Optimizations of Neutral and Zwitterion Species

The predicted energies, dipole moments, volume and polarizability properties computed by using the B3lYP/6-311++G** method are shown for both species in Table 1. Here, it is very important to see the proximities of dipole moments of R1 and R2 despite the different rings present in both structures, in particular in GP, because in solution, the μ values show higher differences between them. Higher polarizabilities are observed for R1 because the phenyl ring is greater than the imidazole one.

Table 1. Calculated total (*E*), dipole moments (μ) and volume (V) for the studied R1 and R2 species in GP and AS.

B3LYP/6-311++G Method**				
GAS (GP)				
Species	E_{ZPVE} (Hartrees)	μ (D)	V (Å^3)	α (a.u.)
R1	-554.77332	5.63	182.0	119.014
R2	-549.30002	5.87	160.5	109.834
AQUEOUS SOLUTION (AS)				
Species	E_{ZPVE} (Hartrees)	μ (D)	V (Å^3)	α (a.u.)
R1	-554.80136	14.73	184.1	172.879
R2	-549.33255	15.69	161.5	154.785

R1: L-phenylalanine, R2: L-imidazolium-alanine

3.2. Vibrational Study of Neutral and Zwitterions Species

The Amino Acid (AA) is as zwitterion even in the solid state, as revealed by Mossou et al. and as reported from many studies. [33, 34,46,47] Hence, in GP calculations, the two AAs are as neutral species containing the NH_2 and COOH groups, while in calculations in aqueous solution, both AAs are optimized as zwitterions where those groups change to NH_3^+ and COO^- groups. [32-34] Then, neutral and zwitterion R1 and R2 species present the same groups, and the only differences are the three deformations and torsions expected for the six-member phenyl ring in R1, while in R2, two deformations and torsions are expected for the imidazole ring. In Figure 2 are shown the predicted IR spectra for neutral R1 and R2 computed at the B3LYP/6-311++G** level of theory in the 4000-0 cm^{-1} region, while Figure 5 shows clear differences in the theoretical IR spectra of R1 and R2 zwitterions due to the NH_3^+ and COO^- groups. In Figures 3 and 4 are shown the same spectra of Figure 2 but in the 4000-0 and 2000-0 cm^{-1} regions, respectively. Figure 3 and 4 show the differences in the positions and intensities of predicted bands. Thus, in the 4000-2000 cm^{-1} region, eleven bands are expected in R1 due to only OH, five aromatic C-H, one aliphatic C-H, two anti-symmetric and symmetric NH_2 and CH_2 and three anti-symmetric and symmetric CH_3 stretching modes and only ten for R2. These spectra evidence that in a serious and rigorous vibrational analysis, the AAs should be differenced. Here, it is essential to explain that the vibrational assignments can only be possible with the experimental IR and/or Raman spectra because the bands observed are assigned to the different vibration modes. Table 2 shows the vibrational assignments for the neutral form of R1 and R2 compared with the experimental data of R1 taken from Ref [48].

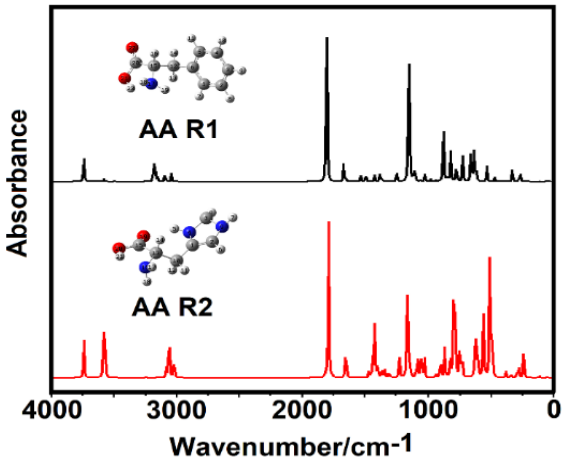

Fig. 2. Predicted IR spectra of neutral forms of R1 and R2.

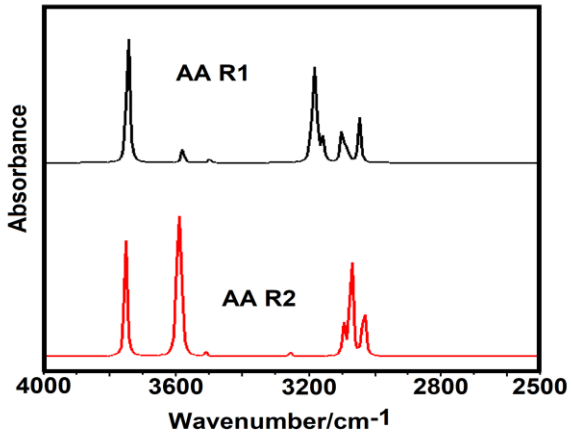

Fig. 3 Predicted IR spectra of neutral R1 and R2 in the 4000-2000 cm-1 region

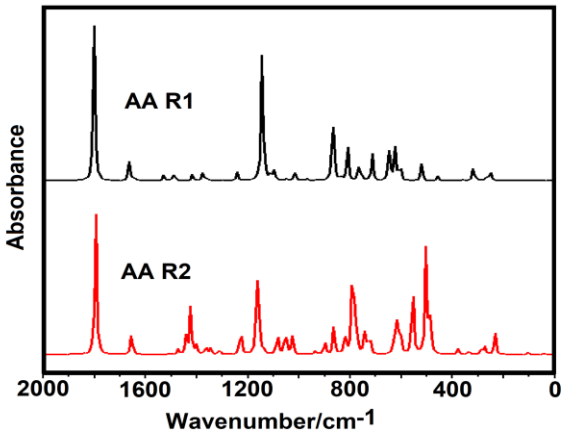

Fig. 4 Predicted IR spectra of neutral R1 and R2 in the 2000-0 cm-1 region

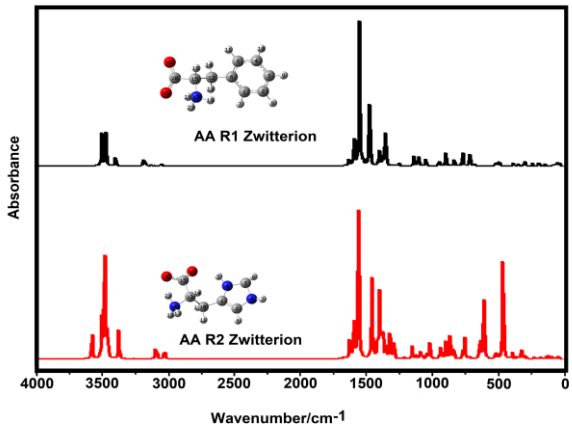

Fig. 5 Predicted IR spectra of zwitterionic forms of R1 and R2

Table 2. Observed and calculated wavenumbers (cm-1) and assignments for neutral forms of R1 and R2.

Experimental[c]		B3LYP/6-311++G** Method[a]			
		GAS (Neutral)			
IR	Raman	R1		R2	
		SQM[b]	Assignments[a]	SQM[b]	Assignments[a]
3446 w		3429	$\nu_a NH_2$	3591	νO20-H21
		3363	$\nu_s NH_2$	3443	$\nu_a NH_2$
3279sh		3334	νO21-H23	3439	νN4-H5
3088m	3089m	3058	νC3-H9	3429	νN9-H7
3067m	3047s	3046	νC4-H10,νC2-H8	3359	$\nu_s NH_2$
3036m		3037	νC3-H9,νC2-H8	3115	νC2-H6
		3025	νC5-H11		
		3022	νC1-H7	2961	νC13-H14
2964m	2971s	2965	$\nu_a CH_2$	2943	$\nu_a CH_2$
	2931s	2918	$\nu_a CH_2$	2940	νC3-H8
2862w		2907	νC15-H16	2902	$\nu_a CH_2$
1626m	1708s	1764	νC20=O22	1724	νC15=O19
1603m	1607s	1589	νC4-C5,νC1-C2		

1564vs	1589s	1588	δNH_2	1612	$\nu C1-C2$
1495s	1541m	1569	$\nu C2-C3,\nu C1-C6,\nu C5-C6$	1579	δNH_2
1456w	1502w	1479	$\beta C4-H10,\beta C2-H8$	1407	δCH_2
1446w	1444m	1440	$\beta C3-H9,\nu C1-C2$	1398	$\rho C13H14\rho' C13H14$
1437w	1426m	1423	δCH_2	1382	$\beta N4-H5$
1411s		1350	$wagCH_2,\delta OH$	1362	$\beta N9-H7$
1406sh	1406sh	1341	δOH	1337	$\rho C13H14\rho' C13H14$
1357sh	1397m	1329	$\rho C15H16,wagCH_2$	1327	$\beta C2-H6,\beta C3-H8$
1336m		1319	$\beta C1-H7$		
1321m		1295	$\nu C4-C5,\nu C1-C6$	1306	$wagCH_2$
1308s	1311s	1260	$\rho' C15H16$	1265	$wagCH_2\delta OH$
1294m	1266w	1246	ρNH_2	1250	$\beta C3-H8$
1237sh	1234w	1186	$\nu C6-C12$	1194	$\nu C1-C10$
1226w	1218m	1169	$\beta C4-H10,\beta C5-H11$	1190	$\beta C2-H6$
1164w	1161vs	1163	$\nu C20-O21$	1125	$\rho NH_2\rho CH_2$
1155w		1150	$\beta C3-H9,\beta C2-H8$	1115	$\nu C15-O20,\delta OH$
1131w		1124	$\rho NH_2,\rho CH_2$	1101	$\nu C3-N9,\nu C3-N4$
1086sh	1073vs	1066	$\nu C15-N17,\nu C1-C2$	1057	$\nu C13-N16$
1075m	1040m	1055	$\nu C15-N17$	1047	$\nu C3-N4$
1028w	1019w	1020	βR_1	1016	$\nu C10-C13$
1025w		996	$\gamma C3-H9$		
	1008w	995	$\beta R_1,\nu C3-C4$	991	$\nu C2-N9,\nu C3-N9$
1007w	977w	977	$\gamma C2-H8$	967	$\beta R_1\nu C1-N4$
996sh		939	$wagNH_2,\delta C20C15N17$		
954w		926	$\gamma C1-H7,\gamma C5-H11$		
915w	915w	915	$\nu C12-C15$	917	$\tau_w CH_2$
907sh	894m	860	$wagNH_2$	885	$\gamma C3-H8$
860sh	843w	848	$\gamma C5-H11,\gamma C1-H7,\gamma C4-H10$	855	βR_2
851m		816	$\tau_w CH_2$	806	γCOO
849m	836s	795	$\nu C15-C20$	771	$wagNH_2$
779m	803w	771	τOH	752	$\nu C13-C15$
746s	751s	747	$\tau R_1,\gamma C3-H9$	731	$\gamma C2-H6$
710sh	733w	710	γCOO	710	$\gamma C2-H6\nu C1-C10$
700s	669s	696	τR_1	614	δCOO
683m	651w	652	δCOO	599	$\gamma C1-C10\tau R_1$
626vw	624m	631	$\beta R_2,\beta R_3$	556	τOH
605w	569w	577	$\beta R_3,\tau R_2$	545	$\gamma N4-H5$
526s	506w	524	ρCOO	496	$\gamma N9-H7$
471w	471s	483	$\gamma C6-C12$	478	ρCOO
422w		401	$\tau R_2,\tau R_3$	368	τR_1
		390	$\delta C12C15N17$	338	τR_2
	351m	347	$\beta C6-C12$	328	$\beta C1-C10$
	323s	326	$\delta C20C15N17$	283	$\delta C10C13N16$
		268	$\tau_w NH_2$	267	$\delta C15C13N16$
	214m	241	$\tau R_3,\tau R_2$	212	$\tau_w NH_2$
	189sh	181	$\delta C20C15C12$	198	$\delta C15C13C10$

		89	δC6C12C15	101	γC1-C10,δC1C10C13
		70	τwCOO	85	τwC10-C1, τC13-C10
		45	τC15-C12	43	τwC10-C1,γN4-H5
		37	τwC12-C6	35	τwCOO

Abbreviations: ν, stretching; β, deformation in the plane; γ, deformation out of plane; wag, wagging; τ, torsion; β_R, deformation ring; τ_R, torsion ring; ρ, rocking; τw, twisting; δ, deformation; a, anti-symmetric; s, symmetric. [a]This work, [b]From the scaled quantum mechanics force field. From Ref [48].

The assignments in the 4000-2000 cm^{-1} region for R1 and R2 show clear differences. When the assignments for the neutral form of R1 are compared with those of its zwitterionic one from Table 3, changes are observed due to the vibration modes of NH_3^+ and COO^- groups. The local symmetry of NH_3^+ is C_{3V}, as the CH_3 groups, while the CH_2 groups present local symmetry C_{2V}. Then, in that region, the zwitterionic forms present two anti-symmetric and one symmetric stretching modes of NH_3^+ and CH_3, while the methylene group's only anti-symmetric and symmetric stretching modes are expected, in addition to the aromatic and aliphatic C-H stretching modes. In the region below 2000 cm^{-1}, two anti-symmetric and one symmetric deformation modes should be assigned for NH_3^+ and CH_3 in addition to the corresponding CH_2 groups and to COO groups. Other rocking and torsion modes of NH_3^+ and CH_3, together with the wagging, rocking and twisting of CH_2, are expected in this region. In the neutral forms in the higher wavenumber region and below 2000 cm^{-1}, differences related to the vibration modes of OH and NH_2 groups are expected. Table S1 (Supporting Material) shows the differences in the assignments of zwitterionic forms of R1 and R2, while Figure S1 (Supporting Material) display comparisons of the experimental IR spectrum of R1 with the corresponding predicted in GP and AS by calculations. As was mentioned above, the vibrational assignments can only be made with the experimental IR and/or Raman spectra. The differences observed are attributed to the calculations because the packing forces observed in the solid state are not considered in the calculations in the gas phase for the isolated molecules.

Table 3. Observed and calculated wavenumbers (cm-1) and assignments for neutral and zwitterion of R1

Experimental[a]		**B3LYP/6-311++G** Method[a]**			
		GAS (Neutral)		**AQUEOUS SOLUTION (Zwitterion)**	
IR	Raman	SQM[b]	Assignments[a]	SQM[b]	Assignments[a]
3446 w		3429	$\nu_a NH_2$	3358	$\nu_a NH_3$
		3363	$\nu_s NH_2$	3327	$\nu_a NH_3$
3279sh		3334	νO21-H23	3257	$\nu_s NH_3$
3088m	3089m	3058	νC3-H9	3060	νC3-H9
3067m	3047s	3046	νC4-H10,νC2-H8	3050	νC4-H10,νC2-H8
3036m		3037	νC3-H9,νC2-H8	3043	νC3-H9,νC1-H7
		3025	νC5-H11	3034	νC1-H7
		3022	νC1-H7	3032	νC5-H11
2964m	2971s	2965	$\nu_a CH_2$	2996	νC15-H16
	2931s	2918	$\nu_a CH_2$	2971	$\nu_a CH_2$
2862w		2907	νC15-H16	2924	$\nu_a CH_2$
1626m	1708s	1764	νC20=O22	1584	νC4-C5,νC1-C2
1603m	1607s	1589	νC4-C5,νC1-C2	1564	νC2-C3,νC1-C6,νC5-C6
1564vs	1589s	1588	δNH_2	1559	$\delta_a NH_3$
1495s	1541m	1569	νC2-C3,νC1-C6,νC5-C6	1524	$\delta_a NH_3$
1456w	1502w	1479	βC4-H10,βC2-H8	1491	νC20=O22
1446w	1444m	1440	βC3-H9,νC1-C2	1473	βC4-H10,βC2-H8
1437w	1426m	1423	δCH_2	1433	βC3-H9,νC1-C2
1411s		1350	$wagCH_2$,δOH	1410	$\delta_s NH_3$

1406sh	1406sh	1341	δOH	1405	δCH_2
1357sh	1397m	1329	ρC15H16, wagCH_2	1362	ρC15H16
1336m		1319	βC1-H7	1350	wagCH_2
1321m		1295	νC4-C5,νC1-C6	1317	βC5-H11,βC1-H7
1308s	1311s	1260	ρ'C15H16	1311	νC20=O21
1294m	1266w	1246	ρNH_2	1288	νC2-C3,νC4-C5
1237sh	1234w	1186	νC6-C12	1250	ρ'C15H16
1226w	1218m	1169	βC4-H10,βC5-H11	1215	ρCH_2
1164w	1161vs	1163	νC20-O21	1184	νC6-C12
1155w		1150	βC3-H9,βC2-H8	1156	βC4-H10,βC2-H8
1131w		1124	ρNH_2,,ρCH_2	1136	βC3-H9
1086sh	1073vs	1066	νC15-N17,νC1-C2	1101	ρNH_3,ρ'C15H16
1075m	1040m	1055	νC15-N17	1068	ρ'NH_3
1028w	1019w	1020	βR_1	1038	ρ'NH_3, ρNH_3
1025w		996	γC3-H9	1017	βR_1
	1008w	995	βR_1,νC3-C4	1015	νC15-N17
1007w	977w	977	γC2-H8	1003	γC3-H9
996sh		939	wagNH_2,δC20C15N17	992	νC3-C4
954w		926	γC1-H7,γC5-H11	988	γC2-H8
915w	915w	915	νC12-C15	926	γC1-H7
907sh	894m	860	wagNH_2	906	νC12-C15,ρNH_3
860sh	843w	848	γC5-H11,γC1-H7,γC4-H10	862	νC15-C20
851m		816	$\tau_w CH_2$	853	γC5-H11,γC4-H10
849m	836s	795	νC15-C20	822	δCOO, $\tau_w CH_2$
779m	803w	771	τOH	798	$\tau_w CH_2$
746s	751s	747	τR_1,γC3-H9	750	τR_1,γC3-H9
710sh	733w	710	γCOO	731	γCOO
700s	669s	696	τR_1	698	τR_1
683m	651w	652	δCOO	667	δCOO
626vw	624m	631	βR_2,βR_3	629	βR_2
605w	569w	577	βR_3,τR_2	570	βR_3
526s	506w	524	ρCOO	508	ρCOO,δC12C15N17
471w	471s	483	γC6-C12	481	τR_2,τR_3
422w		401	τR_2,τR_3	403	τR_2τR_3
		390	δC12C15N17	376	δC12C15N17
	351m	347	βC6-C12	339	βC6-C12
	323s	326	δC20C15N17	295	δC20C15N17,ρCOO
		268	$\tau_w NH_2$	235	τR_3,τR_2
	214m	241	τR_3,τR_2	186	δC20C15C12
	189sh	181	δC20C15C12	130	$\tau_w NH_3$
		89	δC6C12C15	92	δC6C12C15,γC6-C12
		70	τwCOO	62	τwCOO
		45	τC15-C12	45	τC15-C12
		37	τwC12-C6	28	τwC12-C6

Abbreviations: ν, stretching; β, deformation in the plane; γ, deformation out of plane; wag, wagging; τ, torsion; β_R, deformation ring τ_R, torsion ring; ρ, rocking; τ_w, twisting; δ, deformation; a, anti-symmetric; s, symmetric. [a]This work, [b]From the scaled quantum mechanics force field. From Ref [48].

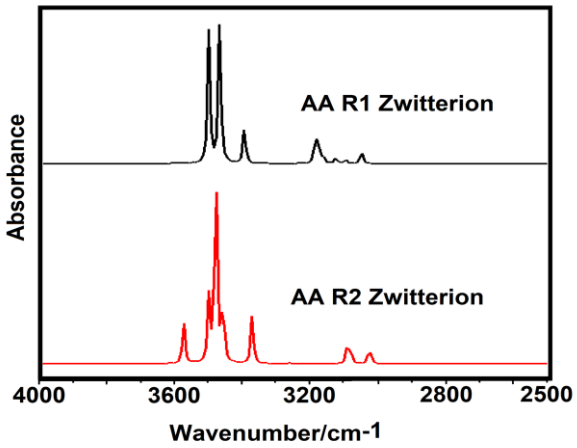

Fig. 6 Predicted IR spectra of zwitterions R1 and R2 in the 4000-2000 cm-1 region

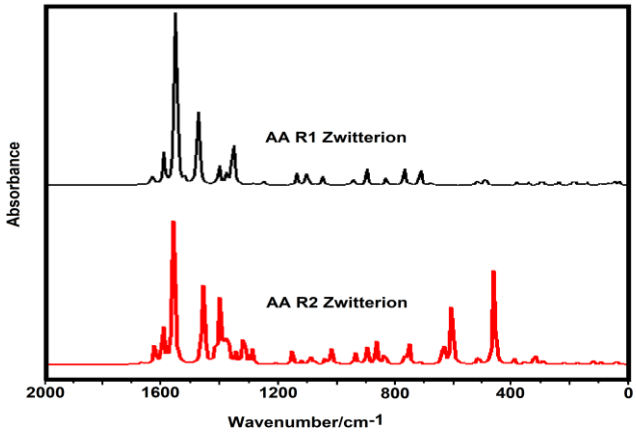

Fig. 7 Predicted IR spectra of zwitterions R1 and R2 in the 2000-0 cm^{-1} region

3.3. Vibrational Study of Chalcons

Phenyl styryl ketones, known as chalcone derivatives, are of medicinal and pharmacological interest because their interesting biological activities are associated with their structures. Thus, two aromatic R1 and R2 rings are connected by an aliphatic chain R1-CO-CH=CH-R2. Therefore, low redox potentials and electron transfer reactions are expected in these species due to the conjugated double bonds and to a completely delocalized π-electron system on both R1 and R2 rings.

[49] Diverse conformations can be present in these species, and, for this reason, the different conformations should be deeply investigated to know the most stable structure, as in the case of 2',4'-dihydroxychalcone isolated from *Zuccagnia punctata* Cav. (Fabaceae) medicinal plant. [49] Figure 8 shows the more stable structures of 2',4'-dihydroxychalcone. Previously, the C1 structure of this chalcone was reported, taking into account only the 1D-NMR, FTIR, UV and mass spectra. [49] However, to perform the vibrational study, the potential energy surface (PES) was studied by using theoretical calculations. Thus, two stable C1 and C2 conformers have been found in the PES, and the presence of the most stable structure C2, different from that of C1 published, was confirmed.

Hence, the combination of experimental 1D-NMR, FTIR, and UV spectra with theoretical calculations is necessary to confirm the correct structure and, after that, to perform the complete vibrational assignments. [49] Full assignments of both conformers shown in Table S2 (Supporting Material) reveal important differences in the

assignments of many vibration modes of both structures and, consequently, theoretical calculations are necessaries to evaluate the conformations when the structure of the species is not determined and confirmed by X-ray diffraction.

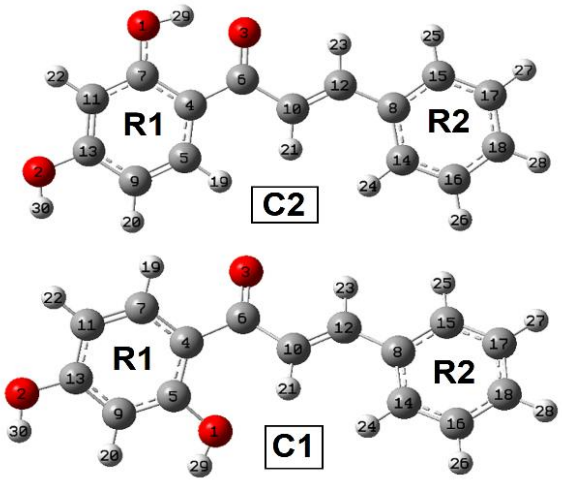

Fig. 8 Stable conformations of 2',4'-dihydroxychalcone isolated from Zuccagnia punctata Cav. (Fabaceae) medicinal plant

3.4. Vibrational Study of Chiral Species

The tropane alkaloid scopolamine is an anticholinergic agent with side effects on the Central Nervous System (CNS), such as memory impairment, confusion, and dementia. [50,51] The structures of free base, cationic and hydrobromide species of this alkaloid present two R and S enantiomers due to chiral carbons. [52] Figure 9 displays the hydrobromide form of scopolamine containing the quaternary N atom with the N-H$^+$···Br$^-$ bond. Hence, the reported vibrational study for these species was performed considering all the possible configurations of these species, as shown in Table S3 (Supporting Material). [52]

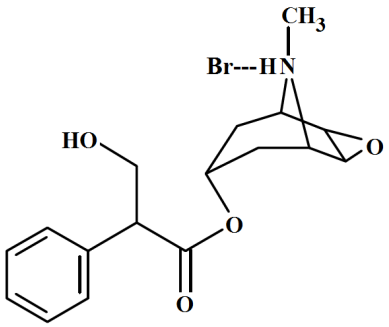

Fig. 9 Molecular structure of the hydrobromide form of scopolamine showing the quaternary N atom with the N-H$^+$···Br$^-$ bond and the N-CH$_3$ group present in all alkaloids

According to the population analyses, the R2 form is present in the free base and hydrobromide forms, while in the cation, the S2 form is present. Hence, the vibrational analyses were performed considering the different configurations of derivatives. [52] Obviously, the positions and intensities of IR bands change due to the ternary and quaternary N atoms present in the free base and cationic and hydrobromide forms, as shown in Table S4. Figure S2 and S3 (Supporting Material) show, respectively, the structures of three species with identifications of rings and comparisons between the experimental FTIR spectrum of hydrobromide of scopolamine in the solid state as tri-hydrate with the predicted for the species in GP at B3LYP/6-31G** level of theory. On the other side, camphor is a cyclic monoterpene ketone and the main component of oil extracted from the wood of the camphor tree, Cinnamomum Camphora (Linne) Nees et Ebermaier family.

This cyclic monoterpene ketone is used in medicinal chemistry due to its anti-inflammatory, analgesic and therapeutics properties. Structures of the two enantiomeric S(-) and R(+) forms of camphor can be seen in Figure 10, while the vibrational assignments are summarized in Table S5 (Supporting Material). [53] Differences in assignments of some vibration modes are clearly observed from that table.

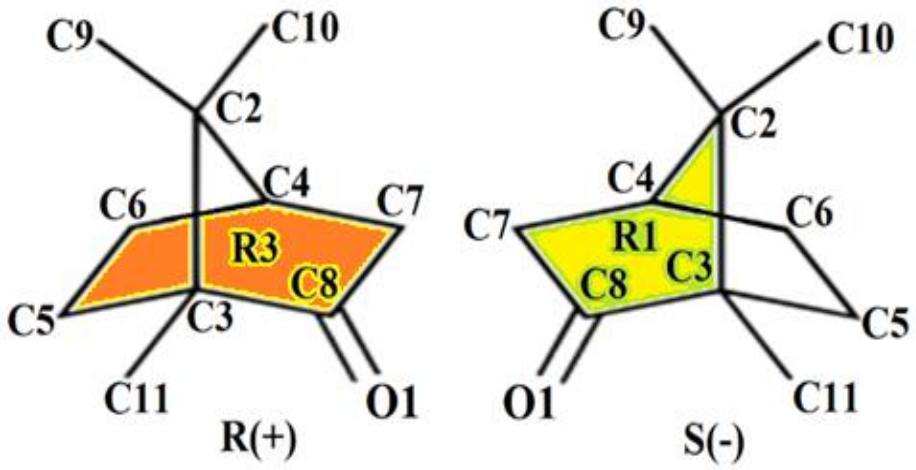

Fig. 10 Molecular structures of S(-) and R(+) forms of camphor with the atom numbering and identification of rings

Complete assignments of expected vibration modes of these types of species only are possible using the internal coordinates, transferable scaling factors and the SQMFF methodology with the Molvib program. [43-45] In chiral molecules, the application of machine learning will be useful and necessary to simplify the huge task that requires obtaining reliable and secure assignments of R and S enantiomers. Thus, the quantity of calculations necessaries to optimize the R and S enantiomers in the different media and, in addition, to perform correct definitions of internal coordinates and assignments of all the vibration modes will be drastically reduced.

3.5. Vibrational Study of the Extract of Plants

Extracts isolated from plants show a wide range of applications in modern medicine and industry because they are used to treat chronic diseases, enhance skin beauty, and provide alternative remedies for various ailments. Besides, their compounds show antioxidant, anti-inflammatory, and antimicrobial properties; some of them are used as corrosion inhibitors. [54, 55] Obviously, the isolation and identification of all its components are crucial steps in their development and use [31]. An example is the case of the extract of *Annona cherimola* that presents multiple components, but the isolation of two acetogenins, squamocin and motrilin, evidenced corrosion inhibitors. [56,57] Previously, the structures of these two components were characterized by using their vibrational spectra. [56,57] Figure 11 shows the molecular structures of the acetogenins squamocin and motrilin. Due to the high number of atoms in the structures of these species (109 atoms), the SQMFF methodology was not applied, and, for this reason, the assignments of main vibrational normal modes of those two species were performed with the aid of the *GaussView* program and of assignments of similar moieties. [58]. Consequently, of the 321 vibration normal modes expected for squamocin, only 129 vibration modes were assigned [56,57]. For the construction of internal coordinates and complete vibrational assignments of this type of species, a machine learning system is needed to simplify the arduous task involved.In another case, the complete structural and vibrational characterization of the sesquiterpene lactone isolated from *mikania parodii* Cabrera and its absolute configuration with an unprecedented spiro connexion were performed by using experimental FT-IR, FTRaman, UV-Visible, ECD, Mass, 1D and 2D-NMR spectra (^{1}H-^{1}H gCOSY, ^{1}H-^{13}C gHSQC, ^{1}H-^{13}C gHMBC, TOCSY and NOESY) combined with B3LYP/6-31G* calculations. The structure of this new dimeric sesquiterpene lactone, parodiolide, can be seen in Figure 12.

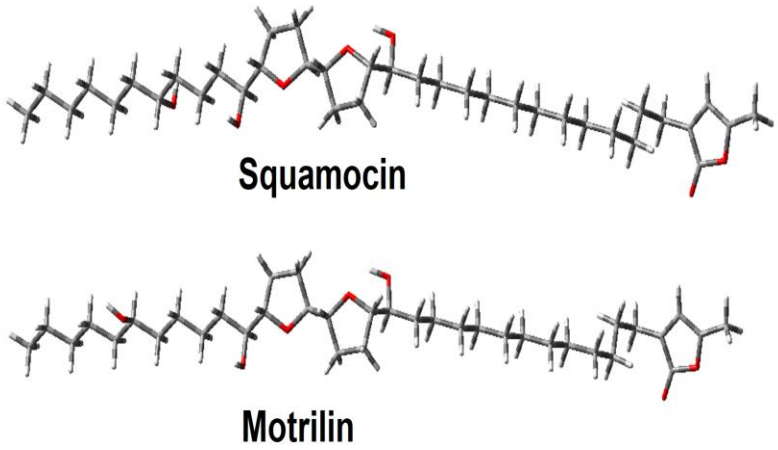

Fig. 11 Molecular structures of acetogenins squamocin and motrilin. Both differ in the position of the OH group linked to the side chains, being -$(CH_2)_5$-CH_3 in squamocin and -$(CH_2)_4$-CH_3 in motrilin

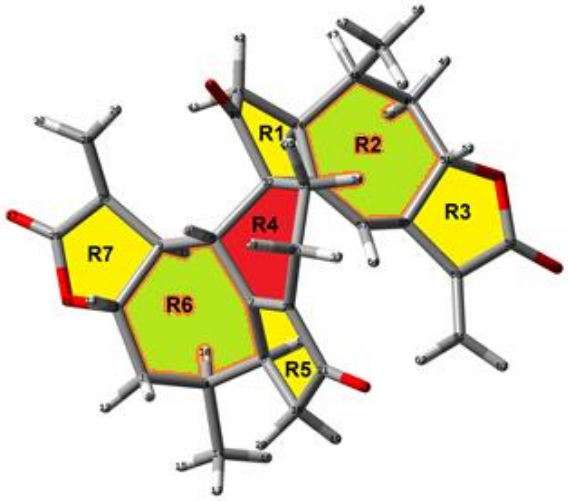

Fig. 12 Structure of dimeric sesquiterpene lactone, parodiolide, a sesquiterpene lactone isolated from mikania parodii Cabrera. Identification of seven rings in different colours

B3LYP/6-31G* calculations optimized paradiolide structures in different media with C_1 symmetry, and due to the presence of 68 atoms in its structure, a total of 198 vibration modes were expected for this species. [59] In this case, the vibrational assignments of all vibration modes are very complicated due to the presence of seven rings, which are shown in different colours in Figure 12, where four present five members (yellow), one of six members (red) and the other two of seven-member rings (green). The complete assignments of vibration modes of paradiolide were performed considering the internal coordinates and transferable scaling factors by using the SQMFF methodology and the Molvib program. [43-45] This study can be seen from Ref. [59]

3.6. Vibrational Study of Nitrate Compounds

Inorganic and hybrid compounds containing the nitrate group are mainly of great interest because their vibrational and chemical properties are strongly related to the coordination modes assumed by nitrate groups. [60-65] Thus, this group is an adaptable ligand that can act as a monodentate or bidentate depending on the type of compound. [60] In the monodentate case, two N=O anti-symmetric and symmetric modes of the $N=O_2$ group and one N-O stretching mode are expected, while in the bidentate mode, one N=O stretching mode and two N-O anti-symmetric and symmetric modes of the $N-O_2$ group. Obviously, the O=N=O deformation mode is different from

those corresponding to the O-N-O angle and, hence, different assignments should be observed for these groups. For those two $N{=}O_2$ and $N{-}O_2$ groups, also are expected wagging, rocking and twisting modes in addition to stretching and deformation modes. Here, it is very important to note that the definitions of normal internal coordinates of these NO_2 groups, where the N atom has hybridization sp^2 with planar structures, are different from those related to the CH_2 group, where the C atom has hybridization sp^3 and a tetrahedral environmental. [37,60-65] The NO_2 group has six normal vibration modes, which are: anti-symmetric and symmetric stretching modes, deformation, wagging, rocking and twisting modes. In chromyl nitrate, both coordination modes can be considered to perform the vibrational analysis, as shown in Figure 13 and Table S6 (Supporting Material). [60] However, the analysis of the scaled force constants computed by using the harmonic force fields presented in Table S7 (Supporting Material) suggests that the coordination mode that better represents the group nitrate in this species is the bidentate one because the obtained values are in agreement with the reported values for this coordination mode.

[60] The latter resulted in defining the coordination mode. In niobyl or vanadyl nitrate (Figure 14), the three nitrate groups can be present as two bidentate and one monodentate (a) and/or as three bidentate (b) ligands. [61,62] The vibrational assignments and the scaled force constants computed are presented in Tables S8 and S9 (Supporting Material). In both niobyl and vanadyl nitrate, bidentate coordination modes are the structures that better represent the nitrate groups of both species. Definitions of normal internal coordinates are shown in those references. [60-65]

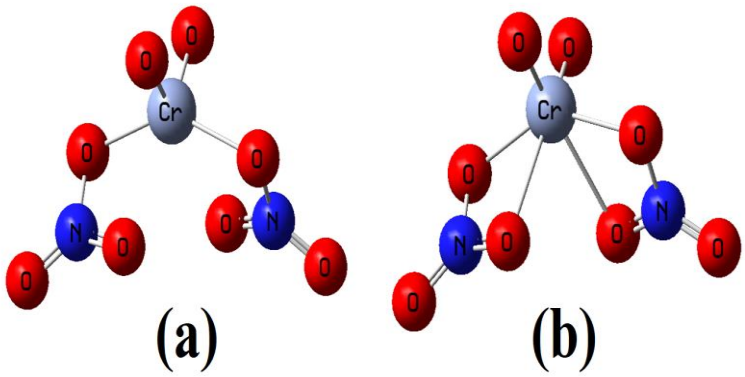

Fig. 13 Structures of chromyl nitrate where the nitrate group is as (a) Monodentate, and (b) bidentate ligands.

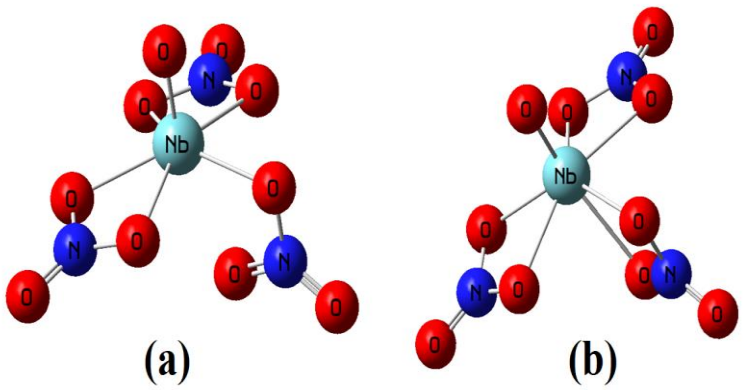

Fig. 14 Structures of niobyl nitrate where the nitrate group is (a) As two bidentate and one monodentate, and (b) As three bidentate ligands.

In hybrid nitrate compounds, such as p-xylylenediaminiumbis(nitrate) and 1,3-Benzenedimethanaminium bis(trioxonitrate) [63,64] and, in an ionic liquid as 1-buthyl-3-methyl imidazolium nitrate [65], the coordination modes of nitrate groups are monodentate, as shown in the Figure 15, 16 and 17, respectively [63-65].

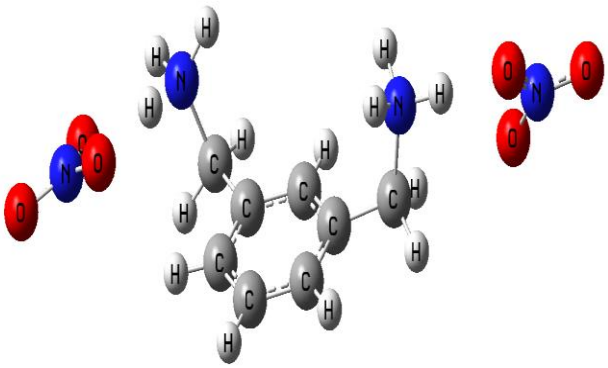

Fig. 15 Structure of p-xylylenediaminiumbis(nitrate)

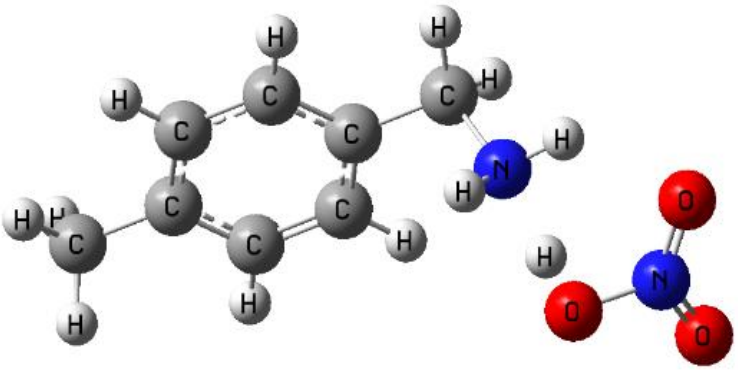

Fig. 16 Structure of 1,3-Benzenedimethanaminium bis(trioxonitrate)

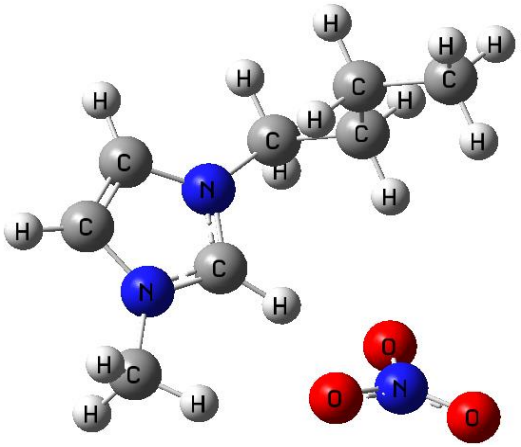

Fig. 17 Structure of 1-buthyl-3-methyl imidazolium nitrate ionic liquid

3.7. Vibrational Study of Phosphate Compounds

Compounds containing phosphate groups are investigated due to their interesting chemical, pharmacological and biochemical properties and mainly because this group is involved in numerous cellular processes as metabolite intermediaries, i.e., in the most abundant phospholipids of all mammalian membranes, phosphatidylcholine and phosphatidylethanolamine, in gluconeogenesis, glycolysis and biosynthesis of essentials aminoacids. [66-70] Then, in vibrational studies of these species and when the normal internal coordinates should be defined, the use of local C_{2v} or C_{3v} symmetries for the phosphate group is indispensable to guarantee reliable and safe vibrational assignments. [66, 68-70] These types of local symmetries for the phosphate group are shown in Figure 18.

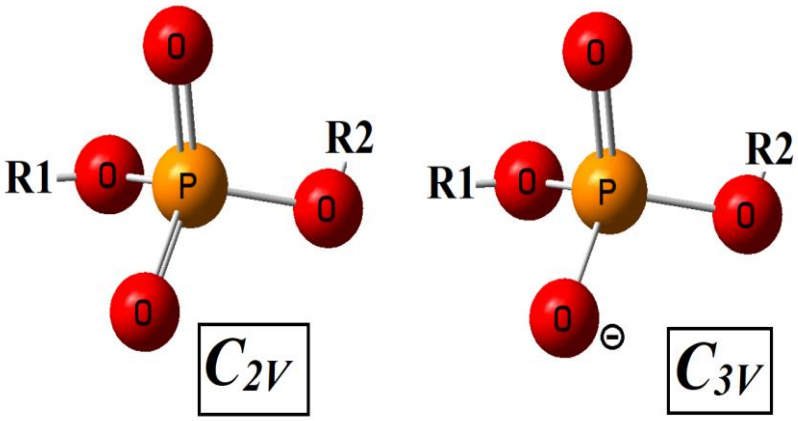

Fig. 18 Structures of phosphate group with (a) local C_{2v}, and (b) local C_{3v} symmetries.

Then, when the C_{2V} symmetry is considered, two different P=O_2 and P-O_2 groups are clearly observed from Figure 18, while if the C_{3V} symmetry is observed, one P=O group and the P-O_3·group are detected.

Thus, the definitions of normal internal coordinates are similar to those defined for the CH_3 group, where nine vibration normal modes are expected: two anti-symmetric and symmetric stretching modes, two anti-symmetric and symmetric deformation modes, two rocking modes and a twisting mode [37, 46, 47, 52, 53, 63, 65]. In the vibrational study of 4-phenylpiperazine-1-ium dihydrogen phosphate, whose structure is shown in Figure 19, for the phosphate group, a C_{2V} symmetry was considered. [70] Thus, two PO_2 and PO_2H groups were observed and assigned in different spectral regions, as given in Table S10 (Supporting Material) [70].

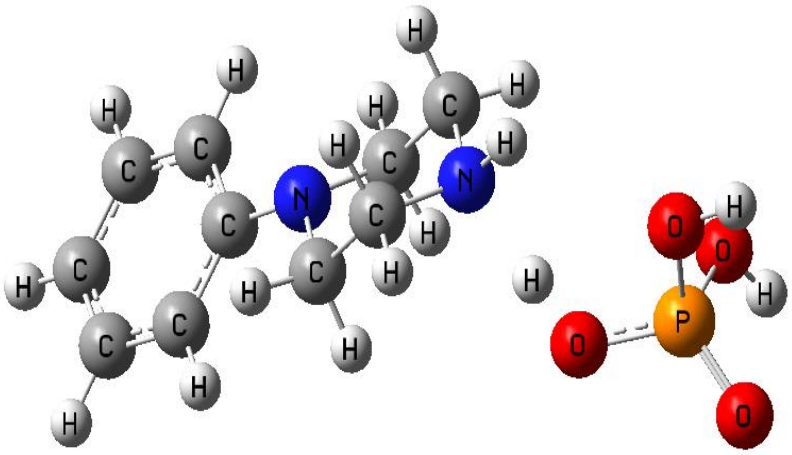

Fig. 19 Structure of 4-phenylpiperazine-1-ium dihydrogen phosphate

On the other side, in the recent study on vibrational assignments of phosphatidylcholine, both local symmetries were considered, although the results revealed that both assignments are reliable and can be used for the identification of the compound, slight differences in the values of scaled force constants are observed when changing the symmetry of the phosphate group. [66] In these cases, comparisons with reported force constants from the literature are necessaries to decide which is the correct symmetry of the phosphate group.

In complexes systems, the application of machine learning will be convenient and essential to shorten the vast job necessary to define the internal coordinates, in particular, those related to large aliphatic side chains and to different types of rings and, obviously, to perform the complete assignments of all the vibration modes.

3.8. Vibrational Study of Hydrated Compounds

Many compounds in the solid state or in solution are present as hydrated species; hence, the anhydrous, monohydrated and di-hydrated structures show differences in their properties, reactivity and behaviours due to the presence of water molecules in their structures. [34, 66, 68, 69, 71-74] Thus, when the structures of hydrated species are known, as in theophylline, violuric acid, Alizarin Red and hydrated tetraphenylphosphonium chloride salt, in the theoretical studies, the water molecules are considered. [71-74] Then, the water molecules show the anti-symmetric and symmetric stretching and deformation modes in addition to the librations modes, which are wagging, rocking and twisting modes.

Thus, the identification of these species by vibrational spectroscopy implies the knowledge of these vibration modes for each water molecule. Figure 20 shows the structure of di-hydrated tetraphenylphosphonium chloride salt, showing the two water molecules and the four rings in different colours, while Table S11 (Supporting Material) shows the complete assignments of anhydrous, monohydrated and di-hydrated species of salt. [74]

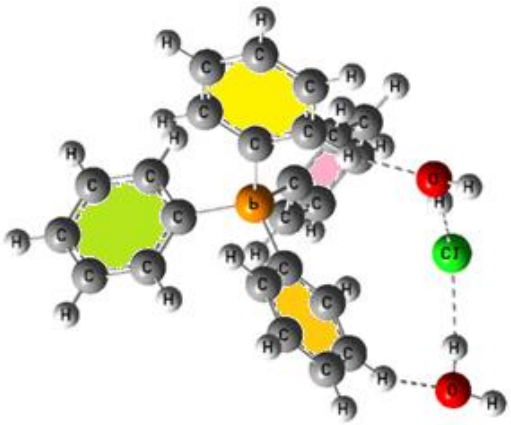

Fig. 20 Structure of di-hydrated tetraphenylphosphonium chloride salt

In complexes systems, the application of machine learning will be convenient and essential to shorten the vast job necessary to define the internal coordinates, in particular, those related to large aliphatic side chains and to different types of rings and, obviously, to perform complete assignments of all the vibration modes.

4. Conclusions

In this investigation, some basics aspects necessaries to assign simple and complexes structures by using the FTIR and Raman spectra combined with the SQMFF methodology have been presented. Structures and vibrational assignments of some AAs, chalcone, chiral components, isolated from plant species, nitrate, phosphate and hydrated compounds have been analysed to show the basics aspects necessaries in machine learning to replace a human expert in vibrational analysis. The use of that approach implies the descriptions of all the normal internal coordinates taking into account the different N-H, OH, CH, CH_2, CH_3, acetate, nitrate, NH_2, NH_3, phosphate groups, different rings and water molecules present in the structures and, obviously, the knowledge of all expected vibration modes. The results show that it is possible to identify neutral and zwitterionic forms of L-phenylalanine from imidazolyl phenylalanine if the vibration modes of six- and five-member rings are performed. In addition, diverse conformers of chalcone can be differentiated when complete assignments of the most stable structures are presented. In chiral species, the R and S structures of enantiomers should be optimized and analysed, and, hence, the vibrational analyses can be performed. However, in components of extract isolated from plants, such as acetogenins, the assignments of all the vibration modes are not possible by using the SQMFF methodology and the Molvib program due to the high number of atoms in their structures. In these cases, only machine learning could

replace a human expert due to the high computational cost involved in the optimizations of structures, studies of potential energy surfaces, and the construction of the internal coordinates. In structures with multiple rings, the greatest difficulty lies in constructing the internal coordinates of different rings. In nitrate species, both coordination monodentate and bidentate modes of nitrate groups should be considered in the assignments; then, the better correlations are observed from the vibrational spectra and the corresponding scaled force constants. In phosphate species, the correct use of a local C_{2v} or C_{3v} symmetry for the phosphate groups is indispensable to assurance consistent and safe vibrational assignments. Complete identifications of hydrated species are performed only when the stretching, deformation, and librations modes (wagging, rocking and twisting) of water molecules are identified and assigned. Vibrational studies related to organic and inorganic compounds present in carbonaceous materials will be addressed in the future.

Data Availability

Data will be made available on request.

Conflicts of Interest

"The author(s) declare(s) that there is no conflict of interest regarding the publication of this paper."

Funding Statement

This work was subsidized with grants from Project N° D714 (Consejo de Investigaciones, Universidad Nacional de Tucumán).

Authors' Contributions

Silvia Antonia Brandán: Conceived and designed the analysis; Analysed and interpreted the data; Wrote the paper, reviewed and edited.

Acknowledgments

The authors thank Prof. Sundius for his permission to use MOLVIB.

Supporting Information available: Tables S1-S11 and Figures S1-S3.

References

[1] Muhammad Zareef et al., "Applications of Benchtop and Portable Spectroscopy Techniques for Food Quality Monitoring," *Spectrochimica Acta Part A: Molecular and Biomolecular Spectroscopy*, vol. 344, 2026. [CrossRef] [Google Scholar] [Publisher Link]

[2] Candela Melendreras et al., "Trends on Vibrational Spectroscopy Tools in the Agri-Food Sector," *Analytical and Bioanalytical Chemistry*, vol. 418, no. 1, pp 15-22, 2025. [CrossRef] [Google Scholar] [Publisher Link]

[3] Art Wei Yao Ang et al., "Analysing the Correlation between the Water's OH Stretching Band and its Hydrogen Bonding Configurations by Machine Learning," *Physical Chemistry Chemical Physics*, vol. 27, no. 39, pp. 21083-21097, 2025. [CrossRef] [Google Scholar] [Publisher Link]

[4] David A. Egger, Manuel Grumet, and Tomáš Bučko, "Machine Learning Accelerates Raman Computations from Molecular Dynamics for Materials Science," *The Journal of Chemical Physics*, vol. 163, no. 12, pp. 1-12, 2025. [CrossRef] [Google Scholar] [Publisher Link]

[5] Piero Lafiosca et al., "Modeling Infrared and Vibrational Circular Dichroism Spectra of Complex Systems: the DFTB/Fluctuating Charges Route," *Physical Chemistry Chemical Physics*, vol. 27, no. 21, pp. 11198-11209, 2025. [CrossRef] [Google Scholar] [Publisher Link]

[6] Junfan Xia, Yaolong Zhang, and Bin Jiang, "The Evolution of Machine Learning Potentials for Molecules, Reactions and Materials," *arXiv preprint*, pp. 1-87, 2025. [CrossRef] [Google Scholar] [Publisher Link]

[7] Ariadni Boziki et al., "A Journey with THeSeuSS: Automated Python Tool for Modeling IR and Raman Vibrational Spectra of Molecules and Solids," *WIREs Computational Molecular Science*, vol. 15, no. 3, pp. 1-16, 2025. [CrossRef] [Google Scholar] [Publisher Link]

[8] Bowen Han et al., "AI-Powered Exploration of Molecular Vibrations, Phonons, and Spectroscopy," *Digital Discovery*, vol. 4, no. 3, pp. 584-624, 2025. [CrossRef] [Google Scholar] [Publisher Link]

[9] Sun Lanjun et al., "Rapid Identification of Marine Microplastics by Laser-Induced Fluorescence Technique based on PCA Combined with SVM and KNN Algorithm," *Environmental Research*, vol. 269, 2025. [CrossRef] [Google Scholar] [Publisher Link]

[10] Shuting Lin et al., "Developing a Fast Fourier Transform Infrared Spectroscopy System for Precise and Reliable Grade Differentiation of *Gastrodia Elata*," *Vibrational Spectroscopy*, vol. 136, 2025. [CrossRef] [Google Scholar] [Publisher Link]

[11] Xiaoyun Huang et al., "Enhancing the Estimation of Cadmium Content in rice Leaves by Integrating Vegetation Indices and Color Indices using Machine Learning," *Ecotoxicology and Environmental Safety*, vol. 290, pp. 1-10, 2025. [CrossRef] [Google Scholar] [Publisher Link]

[12] Luis E. Rodriguez-Saona, and Silvia de Lamo Castellvi, "Vibrational Spectroscopy (Raman and Infrared) and Machine Learning Tools in Food Safety and Composition," *Advances in Food and Nutrition Research*, vol. 115, pp. 165-223, 2025. [CrossRef] [Google Scholar] [Publisher Link]

[13] Stewart F. Parker, "The Analysis of Vibrational Spectra: Past, Present and Future," *ChemPlusChem*, vol. 90, no. 1, pp. 1-15, 2025. [CrossRef] [Google Scholar] [Publisher Link]

[14] Durgesh Ameta et al., "CIRSNet: A Lightweight Chemometric Infrared Spectral Network for Spectral Analysis," *IEEE Transactions on Instrumentation and Measurement*, vol. 74, pp. 1-10, 2025. [CrossRef] [Google Scholar] [Publisher Link]

[15] Wanlin Chen et al., "A Simplified Method for Theoretical Sum Frequency Generation Spectroscopy Calculation and Interpretation: The "pop model," *The Journal of Chemical Physics*, pp. 1-11, 2023. [CrossRef] [Google Scholar] [Publisher Link]

[16] I.A. Boginskaya et al., "Electrochemical Deposition of HSA on Ag Electrode for its Quantitative Determination using SERS and Machine Learning," *Sensors and Actuators A: Physical*, vol. 377, 2024. [CrossRef] [Google Scholar] [Publisher Link]

[17] Jamoliddin Khanifaev, Tim Schrader, and Eva Perlt, "Machine-Learning to Predict Anharmonic Frequencies: A Study of Models and Transferability," *Physical Chemistry Chemical Physics*, vol. 26, no. 35, pp. 23495-23502, 2024. [CrossRef] [Google Scholar] [Publisher Link]

[18] Chengchun Liu, Ruqiang Zou, and Fanyang Mo, "Infrared Spectra Prediction for Functional Group Region Utilizing a Machine Learning Approach with Structural Neighboring Mechanism," *Analytical Chemistry*, vol. 96, no. 39, pp. 15550-15562, 2024. [CrossRef] [Google Scholar] [Publisher Link]

[19] Abir Kebabsa, François Maurel, and Éric Brémond, "Boosting the Modeling of Infrared and Raman Spectra of Bulk Phase Chromophores with Machine Learning," *Journal of Chemical Theory and Computation*, vol. 20, no. 16, pp. 7009-7015, 2024. [CrossRef] [Google Scholar] [Publisher Link]

[20] Ethan Berger et al., "Raman Spectra of Amino Acids and Peptides from Machine Learning Polarizabilities," *Journal of Chemical Information and Modeling*, vol. 64, no. 12, pp. 4601-4612, 2024. [CrossRef] [Google Scholar] [Publisher Link]

[21] Yuzhuo Chen et al., "Accelerating Molecular Vibrational Spectra Simulations with a Physically Informed Deep Learning Model," *Journal of Chemical Theory and Computation*, vol. 20, no. 11, pp. 4703-4710, 2024. [CrossRef] [Google Scholar] [Publisher Link]

[22] Manuel Grumet et al., "Delta Machine Learning for Predicting Dielectric Properties and Raman Spectra," *The Journal of Physical Chemistry C*, vol. 128, no. 15, pp. 6464-6470, 2024. [CrossRef] [Google Scholar] [Publisher Link]

[23] Mandi Fang et al., "Transferability of Machine Learning Models for Predicting Raman Spectra," *The Journal of Physical Chemistry A*, vol. 128, no. 12, pp. 2286-2294, 2024. [CrossRef] [Google Scholar] [Publisher Link]

[24] Mattia Miotto, and Lorenzo Monacelli, "Fast Prediction of Anharmonic Vibrational Spectra for Complex Organic Molecules," *Computational Materials*, vol. 10, no. 1, pp. 1-9, 2024. [CrossRef] [Google Scholar] [Publisher Link]

[25] Manu Krishnan Krishnan Nambudiri et al., "Artificial Intelligence-Assisted Stimulated Raman Histology: New Frontiers in Vibrational Tissue Imaging," *Cancers*, vol. 16, no. 23, pp. 1-29, 2024. [CrossRef] [Google Scholar] [Publisher Link]

[26] Ruocheng Han, Rangsiman Ketkaew, and Sandra Luber, "A Concise Review on Recent Developments of Machine Learning for the Prediction of Vibrational Spectra," *The Journal of Physical Chemistry A*, vol. 126, no. 6, pp. 801-812, 2022. [CrossRef] [Google Scholar] [Publisher Link]

[27] Hao Ren et al., "A Machine Learning Vibrational Spectroscopy Protocol for Spectrum Prediction and Spectrum-Based Structure Recognition," *Fundamental Research*, vol. 1, no. 4, pp. 488-494, 2021. [CrossRef] [Google Scholar] [Publisher Link]

[28] Henry Horst Mantsch, "Biomedical Vibrational Spectroscopy in the Era of Artificial Intelligence," *Molecules*, vol. 26, no. 5, pp. 1-7, 2021. [CrossRef] [Google Scholar] [Publisher Link]

[29] Alexei A. Kananenka et al., "Machine Learning for Vibrational Spectroscopic Maps," *Journal of Chemical Theory and Computation*, vol. 15, no. 12, pp. 6850-6858, 2019. [CrossRef] [Google Scholar] [Publisher Link]

[30] Konstantin E. Dorfman, Frank Schlawin, and Shaul Mukamel, "Nonlinear Optical Signals and Spectroscopy with Quantum Light," *Review os Modern Physics*, vol. 88, no. 4, 2016. [CrossRef] [Google Scholar] [Publisher Link]

[31] Chibuye Bitwell et al., "A Review of Modern and Conventional Extraction Techniques and their Applications for Extracting phytochemicals from Plants," *Scientific African*, vol. 19, pp. 1-19, 2023. [CrossRef] [Google Scholar] [Publisher Link]

[32] Monika Staś, Piotr Najgebauer, and Dawid Siodłak, "Imidazole-Amino Acids. Conformational Switch under Tautomer and pH Change," *Amino Acids*, vol. 55, no. 1, pp. 33-49, 2023. [CrossRef] [Google Scholar] [Publisher Link]

[33] E. Mossou et al., "The Self-Assembling Zwitterionic form of L-Phenylalanine at Neutral pH," *Crystal Structure Communications*, vol. 70, no. 3, pp. 326-331, 2014. [CrossRef] [Google Scholar] [Publisher Link]

[34] Patricio Leyton et al., "An Experimental and Theoretical Study of l-Tryptophan in an Aqueous Solution, Combining Two-Layered ONIOM and SCRF Calculations," *Spectrochimica Acta Part A*: *Molecular and Biomolecular*, vol. 88, pp. 162-170, 2012. [CrossRef] [Google Scholar] [Publisher Link]

[35] J.T. Kloprogge, "Application of Vibrational Spectroscopy in Clay Minerals Synthesis," *Developments in Clay Science*, vol. 8, pp. 222-287, 2017. [CrossRef] [Google Scholar] [Publisher Link]

[36] Sylwia Kukowska, Piotr Nowicki, and Katarzyna Szewczuk-Karpisz, "New Fruit Waste-Derived Activated Carbons of High Adsorption Performance towards Metal, Metalloid, and Polymer Species in Multicomponent Systems," *Scientific Reports*, vol. 15, no. 17, pp. 1-22, 2025. [CrossRef] [Google Scholar] [Publisher Link]

[37] Silvia Antonia Brandán, "MOLVIB vs VEDA. Revealing the Best Program to Generate Safe and Reliable Vibrational Analysis," *Chemical Physics Impact*, vol. 11, pp. 1-11, 2025. [CrossRef] [Google Scholar] [Publisher Link]

[38] Adriana Valls et al., "Imidazole and Imidazolium Antibacterial Drugs Derived from Amino Acids," *Pharmaceuticals*, vol. 13, no. 12, pp. 1-17, 2020. [CrossRef] [Google Scholar] [Publisher Link]

[39] GaussView Version 6.1.1 Release Notes, Expanding the Limits of Computational Chemistry. [Online]. Available: https://gaussian.com/gv611rn/

[40] A.D. Becke, "Density-Functional Exchange-Energy Approximation with Correct Asymptotic Behavior," *Physical Review A*, vol. 38, no. 6, pp. 3098-3100, 1988. [CrossRef] [Google Scholar] [Publisher Link]

[41] Chengteh Lee, Weitao Yang, and Robert G. Parr, "Development of the Colle-Salvetti Correlation-Energy Formula into a Functional of the Electron Density," *Physical Review B*, vol. 37, no. 2, pp. 785-789, 1988. [CrossRef] [Google Scholar] [Publisher Link]

[42] M.J. Frisch et al., "Gaussian 16, Revision C. 01, Gaussian," *Wallingford CT 2016 Inc.*, 2016. [Google Scholar]

[43] Peter Pulay et al., "Combination of Theoretical ab Initio and Experimental Information to Obtain Reliable Harmonic Force Constants. Scaled Quantum Mechanical (QM) Force Fields for Glyoxal, Acrolein, Butadiene, Formaldehyde, and Ethylene," *Journal of the American Chemical Society*, vol. 105, no. 24, pp. 7037-7047, 1983. [CrossRef] [Google Scholar] [Publisher Link]

[44] Guntram Rauhut, and Peter Pulay, "Transferable Scaling Factors for Density Functional Derived Vibrational Force Fields," *The Journal of Physical Chemistry*, vol. 99, no. 10, pp. 3093-3100, 1995. [CrossRef] [Google Scholar] [Publisher Link]

[45] T. Sundius, "Scaling of ab-Initio Force Fields by MOLVIB," *Vibrational Spectroscopy*, vol. 29, no. 1-2, pp. 89-95, 2002. [CrossRef] [Google Scholar] [Publisher Link]

[46] C.D. Contreras et al., "Hydration of L-Tyrosine in Aqueous Medium. An Experimental and Theoretical Study by Mixed Quantum Mechanical/Molecular Mechanics Methods," *Vibrational Spectroscopy*, vol. 57, no. 1, pp. 108-115, 2011. [CrossRef] [Google Scholar] [Publisher Link]

[47] Karina Andrea Guzzetti et al., "Structural and Vibrational Study on Zwitterions of l-Threonine in Aqueous Phase using the FT-Raman and SCRF Calculations," *Journal of Molecular Structure*, vol. 1045, pp. 171-179, 2013. [CrossRef] [Google Scholar] [Publisher Link]

[48] Chemical Book, 2023. [Online]. Available: https://www.chemicalbook.com

[49] Fernanda Corrales Chahar et al., "Experimental and DFT studies on 2',4'-Dihydroxychalcone, A Product Isolated from *ZUCCAGNIA Punctata Cav*. (Fabaceae) Medicinal Plant," *Journal of Molecular Structure*, vol. 1201, 2020. [CrossRef] [Google Scholar] [Publisher Link]

[50] Marjan Gholami, Shadi Sarahroodi, and Saeid Abbasi-Maleki, "Assessment of Gentisic Acid's Protective Effects on Scopolamine-Induced Alzheimer's Disease in Male Mice," *Phytomedicine Plus*, vol. 5, no. 4, pp. 1-10, 2025. [CrossRef] [Google Scholar] [Publisher Link]

[51] Joanna Szala-Rycaj et al., "Neuroprotective Potential of Phytocompounds in the Treatment of Dementia: The State of Knowledge from the Scopolamine-Induced Animal Model of Alzheimer's Disease," *Current Issues in Molecular Biology*, vol. 47, no. 8, pp. 1-20, 2025. [CrossRef] [Google Scholar] [Publisher Link]

[52] Roxana A. Rudyk et al., "Structural, FT-IR, FT-Raman and ECD Spectroscopic studies of Free Base, Cationic and Hydrobromide Species of Scopolamine Alkaloid," *Journal of Molecular Structure*, vol. 1180, pp. 603-617, 2019. [CrossRef] [Google Scholar] [Publisher Link]

[53] José Ruiz Hidalgo, and Silvia Antonia Brandán, "Vibrational Study of S(-) and R(+) Forms of Analgesic Camphor Combining DFT Calculations with Normal Internal Coordinates and SQMFF Methodology," *Journal of Materials and Environmental Science*, vol. 11, no. 9, pp. 1512-1530, 2020. [Google Scholar] [Publisher Link]

[54] Patricia E. Alvarez et al., "*Rollinia Occidentalis* Extract as Green Corrosion Inhibitor for Carbon Steel in HCl Solution," *Journal of Industrial and Engineering Chemistry*, vol. 58, pp. 92-99, 2018. [CrossRef] [Google Scholar] [Publisher Link]

[55] Patricia E. Alvarez et al., "Improved Electrochemical Strategy to Characterize Adsorption and Corrosion Inhibition Related to Biomolecules from Plant Extracts: The Case of *Annona Cherimola*," *Results in Chemistry*, vol. 4, pp. 1-10, 2022. [CrossRef] [Google Scholar] [Publisher Link]

[56] José Ruiz Hidalgo et al., "Experimental Isolation and Spectroscopic Characterization of Squamocin Acetogenin Combining FT-IR, FT-Raman and UV-Vis Spectra with DFT Calculations," *Journal of Molecular Structure*, vol. 1219, 2020. [CrossRef] [Google Scholar] [Publisher Link]

[57] José Ruiz Hidalgo et al., "FT-IR, FT-Raman and UV-Visible Spectra of Motrilin Acetogenin Isolated from *Annona Cherimolia*," *Journal of Molecular Structure*, vol. 1196, pp. 508-517, 2019. [CrossRef] [Google Scholar] [Publisher Link]

[58] GaussView 6, Expanding the Limits of Computational Chemistry. [Online]. Available: https://gaussian.com/gaussview6/

[59] Laura C. Laurella et al., "Structure and Absolute Configuration of Parodiolide, a New Dimeric Sesquiterpene Lactone Isolated from *Mikania Parodii* Cabrera Possessing an Uncommon Spiro Connexion," *Journal of Molecular Structure*, vol. 1253, 2022. [CrossRef] [Google Scholar] [Publisher Link]

[60] Silvia Antonia Brandán et al., "DFT Calculation of the Chromyl Nitrate, $CrO_2(NO_3)_2$: The Molecular Force Field," *Spectrochimica Acta. Part A.: Molecular and Biomolecular Spectroscopy*, vol. 69, no. 3, pp. 1027-1043, 2008. [CrossRef] [Google Scholar] [Publisher Link]

[61] S.A. Brandan et al., "DFT Calculation of the Molecular Force Field of Vanadyl Nitrate, $VO(NO_3)_3$," *Journal of Inorganic and General Chemistry*," vol. 635, no. 3, pp. 582-592, 2009. [CrossRef] [Google Scholar] [Publisher Link]

[62] M.V. Castillo et al., "Theoretical Structural and Experimental Vibrational Study of Niobyl Nitrate," *Journal of Molecular Structure*, vol. 994, no. 1-3, pp. 202-208, 2011. [CrossRef] [Google Scholar] [Publisher Link]

[63] S. Gatfaoui et al., "Synthesis and Characterization of *p*-Xylylenediaminium bis (Nitrate). Effects of the Coordination Modes of Nitrate Groups on their Structural and Vibrational Properties," *Journal of Molecular Structure*, vol. 1151, pp. 152-168, 2018. [CrossRef] [Google Scholar] [Publisher Link]

[64] Sofian Gatfaoui et al., "Deciphering Non-Covalent Interactions of 1,3-Benzenedimethanaminium bis(trioxonitrate): Synthesis, Empirical and Computational Study," *Journal of Molecular Structure*, vol. 1250, 2022. [CrossRef] [Google Scholar] [Publisher Link]

[65] Jonas Kausteklis et al., "Cation-Anion Interactions in 1-Buthyl-3-Methyl Imidazolium Nitrate Ionic Liquid and their Effect on their Structural and Vibrational Properties," *Journal of Molecular Structure*, vol. 1164, pp. 1-14, 2018. [Google Scholar]

[66] Sonia B. Diaz, Davide Romani, and Silvia Antonia Brandán, "Complete Vibrational Assignments of Phosphatidylcholine Combining FTIR and FT-Raman Spectra with DFT and SQMFF Calculations," *Vibrational Spectroscopy*, vol. 143, 2026. [CrossRef] [Google Scholar] [Publisher Link]

[67] Maria del Pilar Buera et al., *Water Properties of Food, Pharmaceutical, and Biological Materials*, 1st ed., CRC Press, Boca Raton, 2006. [CrossRef] [Google Scholar] [Publisher Link]

[68] Silvia Antonia Brandán et al., "Experimental and Theoretical Study of the Hydration of Phosphate Groups in Esters of Biological Interest," *Spectrochimica Acta Part A: Molecular and Biomolecular Spectroscopy*, vol. 66, no. 4-5, pp. 884-897, 2007. [CrossRef] [Google Scholar] [Publisher Link]

[69] Silvia Antonia Brandán et al., "Hydration of Inorganic Phosphates in Crystal Lattices and in Aqueous Solution: An Experimental and Theoretical Study," *Spectrochimica Acta Part A: Molecular and Biomolecular Spectroscopy*, vol. 66, no. 4-5, pp. 1152-1164, 2007. [CrossRef] [Google Scholar] [Publisher Link]

[70] Olfa Noureddine et al., "Experimental and DFT Studies on the Molecular Structure, Spectroscopic Properties, and Molecular Docking of 4-Phenylpiperazine-1-ium Dihydrogen Phosphate," *Journal of Molecular Structure*, vol. 1207, 2020. [CrossRef] [Google Scholar] [Publisher Link]

[71] Davide Romani, and Silvia Antonia Brandán, "Investigating the Role of Water Molecules and its Impact on the Properties of Hydrated Vasodilator and Anti-Asthmatic Theophylline Agent," *Computational and Theoretical chemistry*, vol. 1231, 2024. [CrossRef] [Google Scholar] [Publisher Link]

[72] Maximiliano A. Iramain et al., "Vibrational Assignments of Monohydrate Dimer of Violuric Acid by using FT-IR, FT-Raman and UV Spectra and DFT Calculations in Different Media," *Journal of Molecular Liquids*, vol. 409, 2024. [CrossRef] [Google Scholar] [Publisher Link]

[73] César A.N. Catalán et al., "Structural and Vibrational Characterizations of Alizarin Red S," *Molecules*, vol. 30, no. 15, pp. 1-20, 2025. [CrossRef] [Google Scholar] [Publisher Link]

[74] Annalisa Paolone, and Silvia Antonia Brandán, "Structural and Harmonic Force Fields Studies of Anhydrous, Mono and Dihydrated Tetraphenylphosphonium Chloride Salts for Ionic Liquids," *Journal of Molecular Liquids*, vol. 447, 2026. [CrossRef] [Google Scholar] [Publisher Link]

Appendix

Table S1. Observed and calculated wavenumbers (cm^{-1}) and assignments for zwitterionic forms of R1 and R2.

Experimental[c]		B3LYP/6-311++G** Method[a] AQUEOUS SOLUTION (Zwitterion)			
		R1		R2	
IR	Raman	SQM[b]	Assignments[a]	SQM[b]	Assignments[a]
				3429	νN9-H7
3446 w		3358	$\nu_a NH_3$	3358	$\nu_a NH_3$
		3327	$\nu_a NH_3$	3338	νN4-H5
				3317	$\nu_a NH_3$
3279sh		3257	$\nu_s NH_3$	3235	$\nu_s NH_3$
3088m	3089m	3060	νC3-H9	3128	νC2-H6
3067m	3047s	3050	νC4-H10,νC2-H8		
3036m		3043	νC3-H9,νC1-H7		
		3034	νC1-H7		
		3032	νC5-H11	2969	νC13-H14
2964m	2971s	2996	νC15-H16	2964	νC3-H8
	2931s	2971	$\nu_a CH_2$	2953	$\nu_a CH_2$
2862w		2924	$\nu_a CH_2$	2902	$\nu_a CH_2$
1626m	1708s	1584	νC4-C5,νC1-C2	1611	νC1-C2
1603m	1607s	1564	νC2-C3,νC1-C6,νC5-C6		
1564vs	1589s	1559	$\delta_a NH_3$	1553	$\delta_a NH_3$
1495s	1541m	1524	$\delta_a NH_3$	1527	$\delta_a NH_3$
1456w	1502w	1491	νC20=O22	1498	νC15=O19,νC15=O20
1446w	1444m	1473	βC4-H10,βC2-H8		
1437w	1426m	1433	βC3-H9,νC1-C2	1397	$\delta_s NH_3$
1411s		1410	$\delta_s NH_3$	1393	δCH_2
1406sh	1406sh	1405	δCH_2	1374	$\delta_s NH_3$,ρC13H14
1357sh	1397m	1362	ρC15H16	1343	βN9-H7
1336m		1350	$wagCH_2$	1338	ρC13H14, $wagCH_2$
1321m		1317	βC5-H11,βC1-H7	1330	ρ'C13H14, νC13-C15
1308s	1311s	1311	νC20=O21	1311	βC2-H6,$wagCH_2$
1294m	1266w	1288	νC2-C3,νC4-C5	1281	ρ'C13H14, νC15=O20
1237sh	1234w	1250	ρ'C15H16	1251	βC3-H8
1226w	1218m	1215	ρCH_2	1193	βC2-H6
1164w	1161vs	1184	νC6-C12	1177	ρCH_2
1155w		1156	βC4-H10,βC2-H8		
1131w		1136	βC3-H9	1120	ρNH_3,ρ'C13H14
1086sh	1073vs	1101	ρNH_3,ρ'C15H16	1084	νC3-N9
1075m	1040m	1068	ρ'NH_3	1064	ρ'NH_3
1028w	1019w	1038	ρ'NH_3 ρNH_3		
1025w		1017	βR_1		
	1008w	1015	νC15-N17	1040	νC3-N4
1007w	977w	1003	γC3-H9	999	νC13-N16
996sh		992	νC3-C4	985	νC2-N9
954w		988	γC2-H8	965	νC3-N9,νC1-N4
915w	915w	926	γC1-H7	910	νC10-C13
907sh	894m	906	νC12-C15,ρNH_3	887	γC3-H8
860sh	843w	862	νC15-C20	876	$\tau_w CH_2$,γC3-H8
851m		853	γC5-H11,γC4-H10	855	βR_2

849m	836s	822	δCOO, $\tau_w CH_2$	807	δCOO, $\tau_w CH_2$νC13-C15
779m	803w	798	$\tau_w CH_2$	749	γC2-H6,γCOO
746s	751s	750	τR_1,γC3-H9	736	γC2-H6,$\tau_w CH_2$
710sh	733w	731	γCOO	702	νC1-C10
700s	669s	698	τR_1	623	γN4-H5,γC1-C10
683m	651w	667	δCOO	598	γN4-H5βR_1
626vw	624m	629	βR_2	566	τR_1γC1-C10
605w	569w	570	βR_3	506	ρCOO
526s	506w	508	ρCOO,δC12C15N17	457	γN9-H7
471w	471s	481	$\tau R_2\tau R_3$	383	$\tau R_1\tau R_2$
422w		403	$\tau R_2\tau R_3$	350	δC15C13C10,βC1-C10
		376	δC12C15N17	322	ρCOO, βC1-C10
	351m	339	βC6-C12	319	δC10C13N16,δC15C13N16
	323s	295	δC20C15N17,ρCOO	288	τR_2,γN4-H5
		235	τR_3,τR_2	219	δC15C13C10,βC1-C10
	214m	186	δC20C15C12	155	$\tau_w NH_3$
	189sh	130	$\tau_w NH_3$	119	γC1-C10,δC1C10C13
		92	δC6C12C15,γC6-C12	86	τwC10-C1
		62	τwCOO	52	τwCOO
		45	τC15-C12	40	τC13-C10
		28	τwC12-C6		

Abbreviations: ν, stretching; β, deformation in the plane; γ, deformation out of plane; wag, wagging; τ, torsion; β_R, deformation ring τ_R, torsion ring; ρ, rocking; τw, twisting; δ, deformation; a, antisymmetric; s, symmetric. [a]This work, [b]From scaled quantum mechanics force field. [c]From Ref [48].

Table S2. Observed and calculated wavenumbers (cm^{-1}) and assignments for C1 and C2 of 2′,4′-dihydroxychalcone in gas phase by using the B3LYP/6-311++G Method.**

Experimental	B3LYP/6-311++G** Method[a]			
IR	C2		C1	
	SQM[b]	Assignments	SQM[b]	Assignments
3340s	3672	νO2-H30	3675	νO1-H29
3340s	3086	νC10-H21	3674	νO2-H30
3108sh	3076	νC11-H22	3092	νC10-H21
3085s	3071	νO1-H29	3075	νC11-H22
3066s	3065	νC5-H19	3063	νC7-H19
	3061	νC16-H26	3060	νC18-H28
	3054	νC14-H24	3054	νC14-H24,νC17-H27
	3046	νC18-H28	3045	νC18-H28,νC15-H25
	3038	νC15-H25	3036	νC15-H25,νC16-H26
3032s	3033	νC9-H20	3031	νC17-H27,νC18-H28
2901sh	3033	νC17-H27	3020	νC12-H23
2926sh	3023	νC12-H23	3003	νC9-H20
1635vs	1627	νC10=C12	1650	νC6=O3,νC10=C12
1615s	1611	νC5-C9,νC7-C11	1595	νC7-C11
1592s	1586	νC14-C16	1588	νC14-C16
1575s	1562	νC8-C15	1578	νC13-C11,νC10=C12
1567s	1559	νC13-C11	1566	νC9-C13

1558s	1547	νC6=O3	1557	νC17-C18
1515s	1485	βC5-H19	1489	βC9-H20
1497s	1479	βC16-H26	1479	βC16-H26,βC14-H24
1448s	1436	βC18-H28,βC17-H27	1436	βC18-H28,βC17-H27
1440sh	1418	νC7-O1	1423	νC5-C9
1361vs	1377	δO1-H29	1328	βC10-H21
1325m	1344	βC10-H21	1321	βC10-H21
1319sh	1326	βC14-H24	1314	νC4-C5
1303s	1316	νC13-O2	1306	βC12-H23
1287s	1302	βC12-H23	1296	βC7-H19
1279sh	1292	νC4-C7	1271	νC8-C14
1250sh	1267	νC8-C12,νC8-C14	1252	νC4-C7,νC13-O2
1229s	1222	νC4-C5	1194	νC8-C12,νC8-C15
1215s	1196	νC4-C6,νC8-C12	1185	νC4-C6
1185m	1193	βC12-H23,βC10-H21	1170	νC5-O1
1174sh	1178	βC11-H22	1168	βC15-H25
1150sh	1170	βC15-H25	1150	βC18-H28,βC17-H27
1140s	1151	βC18-H28,βC17-H27	1142	δO1-H29
1140s	1142	βC9-H20	1128	δO2-H30
1084w	1122	δO2-H30	1082	βC11-H22
1072w	1069	νC15-C17	1068	νC15-C17
1044sh	1022	γC12-H23	1020	γC12-H23
1033m	1016	νC18-C16,νC17-C18	1017	νC18-C16
1023m	1009	νC6-C10	1015	νC6-C10
1000m	992	βR_1(A2)	993	βR_1(A2)
1000m	990	γC18-H28,γC17-H27	990	γC18-H28,γC17-H27
986sh	972	γC16-H26	981	γC7-H19
976s	954	νC9-C13	974	γC16-H26
940vw	922	γC15-H25	961	νC13-C11
919w	909	γC5-H19	922	γC15-H25
887w	884	νC8-C14	892	γC10-H21
859m	868	γC10-H21	884	δC6C10C12,νC8-C14
841sh	846	γC11-H22	839	γC14-H24
836m	837	γC14-H24	829	γC11-H22
807w	781	βR_2(A2),βC6=O3	791	γC9-H20
791w	779	γC6=O3	776	βR_2(A2),νC8-C12
767m	772	τO1-H29,γC9-H20	764	τR_1(A2), γC18-H28
750w	755	τR_1(A2),γC18-H28	738	βR_1(A1)
735m	739	βR_2(A1)βR_1(A1)	729	γC6=O3
692m	716	τR_1(A1), γC6=O3	682	τR_1(A2)
673m	679	τR_1(A2)	663	τR_1(A1)
663w	654	τR_1(A1)	630	βR_3(A2)
	632	γC13-O2,γC7-O1	628	γC13-O2,γC5-O1
	629	βR_3(A2)	621	βR_3(A1), γC5-O1
	624	βR_3(A1), βR_2(A2)	579	βR_2(A2)

592	βC4-C6,βC7-O1	560	βC6=O3
575	βR_2(A2),βC6=O3	534	βR_2(A1), βR_3(A1)
524	δC4C6C10	486	γC8-C12
485	βC7-O1	468	βC8-C12
484	τR_3(A2),γC8-C12	448	τR_2(A1), τR_3(A1)
438	τR_3(A1)	398	τR_2(A2)
399	βR_3(A1)	388	βC13-O2
396	τR_2(A2)	338	βC5-O1
374	βC13-O2	311	γC4-C6
326	βC4-C6	288	τO2-H30
309	τO2-H30	285	τO1-H29
273	γC4-C6	264	τO1-H29,γC4-C6
258	τR_3(A2),τC10-C12	259	τR_3(A2)
217	τR_3(A1),τR_2(A1)	213	τR_3(A1),τR_1(A1)
198	δC6C10C12,νC4-C6	200	δC6C10C12,νC4-C6
183	βC8-C12	194	βC4-C6
107	τR_2(A1),τC6-C10	111	τR_2(A1), τC6-C10
100	τC10-C12	88	τC10-C12
73	τ_wC12-C8	77	τ_wC12-C8,τC6-C10
55	δC6C10C12,δC8C12C10	50	δC6C10C12,δC8C12C10,δC4C6C10
24	τ_wC6-C4	22	τ_wC6-C4
13	τ_wC12-C8	18	τC6-C10,τ_wC12-C8

Abbreviations: ν, stretching; β, deformation in the plane; γ, deformation out of plane; wag, wagging; τ, torsion; β_R, deformation ring τ_R, torsion ring; ρ, rocking; τw, twisting; δ, deformation; a, antisymmetric; s, symmetric. [a]This work, [b]From scaled quantum mechanics force field; [c]From B3LYP/6-311++G** calculation.

Table S3. Calculated total (*E*) and relative energies (⚜*E*), dipole moments (μ), volume (V) and populations for the three forms of scopolamine in gas and aqueous solution phases.

B3LYP/6-31G*					
Scopolamine free base					
GAS					
Species	E (Hartrees)	μ (D)	V (Å^3)	ΔE (kJ/mol)	Population %
R1	-1016.0420	2.27	325.0	-17.05	0.01
R2	-1016.0485	2.39	319.0	0.00	97.88
S1	-1016.0441	2.78	324.5	-11.54	0.87
S2	-1016.0447	2.79	321.7	-9.97	1.94
PCM					
Species	E (Hartrees)	μ (D)	V (Å^3)	ΔE (kJ/mol)	Population%
R1	-1016.0670	3.36	324.3	-8.92	1.36
R2	-1016.0704	2.68	320.0	0.00	50.33
S1	-1016.0693	4.52	322.0	-2.88	15.60
S2	-1016.0700	4.14	320.3	-1.05	32.71
Scopolammonium cationic					
GAS					
Species	E (Hartrees)	μ (D)	V (Å^3)	ΔE (kJ/mol)	Population%

R1	-1016.4119	16.44	324.2	-52.46	0.00
R2	-1016.4291	13.52	322.5	-7.34	4.80
S1	-1016.4278	13.09	321.4	-10.75	1.22
S2	-1016.4319	13.66	336.0	0.00	93.98
			PCM		
Species	E (Hartrees)	μ (D)	V (Å^3)	ΔE (kJ/mol)	Population%
R1	-1016.5340	18.79	324.9	-11.80	0.73
R2	-1016.5364	16.46	322.3	-5.51	9.49
S1	-1016.5355	15.93	324.9	-7.87	3.54
S2	-1016.5385	17.79	330.2	0.00	86.24
			Scopolamine hydrobromide		
			GAS		
Species	E (Hartrees)	μ (D)	V (Å^3)	ΔE (kJ/mol)	Population%
R1	-3588.3588	6.71	348.9	49.31	freq (-)
R2	-3588.3776	6.13	348.2	0.00	100.00
S1	-3588.3608	5.14	347.0	44.07	freq (-)
S2	-3588.3395	10.06	359.0	99.94	freq (-)
			PCM		
Species	E (Hartrees)	μ (D)	V (Å^3)	ΔE (kJ/mol)	Population%
R1	-3588.4128	9.39	351.5	5.51	6.86
R2	-3588.4149	9.46	350.0	0.00	62.93
S1	-3588.4142	7.43	354.5	1.84	29.89
S2	-3588.4099	13.80	359.8	13.11	0.32

Table S4. Observed and calculated wavenumbers (cm^{-1}) and assignments for the free base, cationic and hydrobromide species of scopolamine.

Experimental[a]		B3LYP/6-31G* Method[a]					
		Hydrobromide		Cationic		Free base	
IR	Raman	SQM[b]	Assignments[a]	SQM[b]	Assignments[a]	SQM[b]	Assignments[a]
3595br		3570	νO4-H40	3593	νO4-H40	3556	νO4-H40
3350s		3096	$\nu_a CH_3$	3300	νN5-H44		
	3355vw	3080	νC20-H41	3114	$\nu_a CH_3$		
3260sh	3311vw	3069	νC21-H42	3084	νC22-H43	3078	νC22-H43, νC20-H41
	3194vw	3065	ν_sC-H(C6,C7)	3081	ν_sC-H(C6,C7)	3067	νC21-H42
	3163vw	3061	νC22-H43	3073	νC20-H41	3059	νC22-H43,νC18-H38
	3080m	3055	ν_aC-H(C6,C7)	3073	ν_aC-H(C6,C7)	3049	νC18-H38
	3073sh	3053	νC18-H38	3065	νC21-H42	3046	νC19-H39
3047m	3050m	3048	νC19-H39	3053	νC18-H38	3039	ν_sC-H(C6,C7)
	3043sh	3044	$\nu_a CH_3$	3052	$\nu_a CH_3$		
	3034sh	3004	ν_sC-H(C8,C9)	3048	νC19-H39	3027	ν_aC-H(C6,C7)
	3007w	3001	ν_aC-H(C8,C9)	3008	ν_sC-H(C8,C9)		
	3002sh	3000	$\nu_a CH_2$(C11)	3007	$\nu_a CH_2$(C11)		
				3005	ν_aC-H(C8,C9)	2999	$\nu_a CH_2$(C11), νC12-H31
				2998	$\nu_a CH_2$(C16)	2990	$\nu_a CH_2$(C11), $\nu_a CH_2$(C10)
		2993	$\nu_a CH_2$(C10)	2995	$\nu_a CH_2$(C10)	2984	$\nu_a CH_2$(C16)
	2971s	2989	$\nu_a CH_2$(C15)	2978	νC12-H31	2982	$\nu_a CH_3$
	2971s	2976	νC12-H31			2976	νC12-H31
	2971s	2971	$\nu_s CH_3$	2973	$\nu_s CH_3$	2972	ν_sC-H(C8,C9)

	2964sh					2969	ν_aC-H(C8,C9)
2949m	2946sh	2955	νC15-H35	2955	νC15-H35	2968	$\nu_a CH_3$
		2944	$\nu_s CH_2$(C11)	2937	$\nu_s CH_2$(C10)	2944	νC15-H35
	2932w	2940	$\nu_s CH_2$(C10)	2934	$\nu_s CH_2$(C11)	2942	$\nu_s CH_2$(C11)
	2923sh	2911	$\nu_s CH_2$(C15)	2923	$\nu_s CH_2$(C16)	2931	$\nu_s CH_2$(C10)
2886sh	2889w					2907	$\nu_s CH_3$
	2866w					2901	$\nu_s CH_2$(C16)
		1882	νN5-H44				
1739vs	1732w	1712	νC14-O3	1736	νC14-O3	1710	νC14-O3
1696w						1610	νC19-C21,νC18-C20
1606w	1598m	1609	νC19-C21	1599	νC19-C21,νC18-C20	1590	νC20-C22,νC17-C18 νC17-C19
1595sh	1582w 1575vw	1591	νC20-C22	1583	νC20-C22,νC21-C22 νC17-C18		
	1557vw	1526	ρN5-H44 δBr45H44N5				
1494w		1499	βC20-H41	1479	βC20-H41	1499	βC20-H41 βC19-H39
1494w				1478	$\delta_a CH_3$	1487	$\delta_a CH_3$
1475m	1474w			1473	ρN5-H44		
1470m		1471	$\delta_a CH_3$				
1458m		1459	δCH_2(C15)				
1458m		1459	βC22-H43,νC18-C20			1459	βC22-H43,νC18-C20
1458m	1457w	1458	δCH_2(C10)	1457	δCH_2(C16)	1458	δCH_2(C16)
1458m		1455	δCH_2(C11)	1456	δCH_2(C11)	1454	δCH_2(C10)
1442m				1452	δCH_2(C10)	1447	$\delta_a CH_3$
1442m		1441	$\delta_a CH_3$	1443	βC22-H43,νC18-C20	1442	δCH_2(C11)
1436sh	1436w			1427	$\delta_a CH_3$	1424	$\delta_s CH_3$
1425sh	1425w	1416	ρC12-H31 $wagCH_2$(C10)				
1406w	1402w	1411	ρ'N5-H44,τH44-N5	1414	δsCH3,βN5-H44		
1406w	1402w	1406	$wagCH_2$(C15), $\delta_s CH_3$	1404	ρC12-H31	1408	$wagCH_2$(C16)
1406w	1402w	1404	$wagCH_2$(C15)	1400	$wagCH_2$(C16)		
1385m	1385vw	1385	$\delta_s CH_3$	1385	$\delta_s CH_3$	1396	ρC12-H31
1385m	1385vw			1384	ρ'N5-H44	1383	$\delta_s CH_3$νC6-C7
1375sh	1370w	1375	ρ'C12-H31			1372	ρ'C12-H31
1375sh	1370w	1368	ρCH_2(C15)	1365	ρCH_2(C16)	1366	ρCH_2(C16)
	1360w	1353	$wagCH_2$(C11)	1358	$wagCH_2$(C10)		
1350m		1346	βC18-H38			1347	ρC15-H35,βC18-H38
1344sh	1346w					1344	ρC9-H26
		1335	ρC9-H26	1339	ρC15-H35	1335	$wagCH_2$(C11)
		1334	ρC8-H25	1332	$wagCH_2$(C11)	1331	$wagCH_2$(C10)
1327w	1327w			1327	ρC9-H26		
		1328	ρC15-H35	1326	ρC8-H25	1323	ρC15-H35
				1312	βC18-H38 βC19-H39		
1308w	1308w	1309	νC17-C18νC17-C19	1305	νC17-C19	1306	ρ'C15-H35,νC17-C18
1299sh	1298sh					1288	ρC8-H25
	1292sh	1293	ρ'C6-H23	1293	ρ'C7-H24	1284	ρCH_2(C10)
		1283	ρ'C8-H25	1283	ρ'C8-H25	1283	ρ'C7-H24,ρ'C6-H23
1270sh	1273vw	1271	ρ'C7-H24	1269	ρ'C9-H26 ρ'C6-H23		
1262w		1262	ρCH_2(C10)ρCH_2(C11)			1253	ρ'C8-H25ρ'C9-H26
1245w	1246w	1252	ρ'C9-H26	1241	ρCH_2(C11)	1248	ρCH_2(C11)
1245w	1246w					1237	νC14-O2,δCOO

1232sh	1233w	1234	ρ'C15-H35	1229	ρ'C15-H35	1234	ρ'C15-H35
	1230sh	1226	νC14-O2	1225	ρ'N5-H44		
1223m		1213	ρC7-H24 ρC6-H23	1211	τR_1(A2),ρC6-H23	1213	ρ'CH_3
1203w	1206sh	1204	ρ'CH_3 ρ'C9-H26	1201	ρCH_2(C16)δOH	1205	ρC7-H24 ρC6-H23
1184sh	1183sh	1183	βC18-H38, βC19-H39	1185	ρ'CH_3	1182	βC18-H38
	1179m	1172	νC15-C17			1176	νC15-C17
1168vs		1161	βC22-H43, βC21-H42	1165	βC18-H38, βC19-	1164	ρCH_2(C16),δOH
1168vs		1160	δOH	1164	νC15-C17	1161	βC22-H43,βC21-H42
1157sh	1154w			1145	βC22-H43, βC21-	1145	ρCH_2(C11)
	1141w	1143	ρ'CH_3	1143	ρCH_3		
		1141	ρCH_3	1138	ρ'CH_3 ρCH_2(C10)		
1135s				1135	νC14-O2,δCOO	1132	νN5-C13
1116sh	1116w	1097	νC10-C12νC11-C12			1129	ρCH_3
1082sh	1086w	1081	νC18-C20	1092	νC10-C12,νC11-C12	1099	νC10-C12,νC11-C12
1078w		1079	ρC7-H24, ρC6-H23	1078	τR_1(A2)	1080	νC18-C20,νC19-C21
	1070w			1076	ρC6-H23 ρC7-H24		
1068m		1071	τR_1(A2), τR_2(A2)	1071	τR_1(A2), νC18-C20	1071	ρC7-H24, ρC6-H23
1068m		1063	τR_1(A2), τR_2(A2)			1056	τR_1(A2), τR_2(A2)
1047s		1052	νC15-C16	1052	τR_1(A2), τR_2(A2)	1052	νC16-O4,τR_1(A2)
1047s	1047w	1044	νC16-O4	1047	νC16-O4	1046	νC16-O4,νC15-C16
1036sh				1040	νC15-C16	1029	τR_2(A2)
		1027	νC21-C22			1027	βR_1(A1)νC21-C22
	1027m	1020	νN5-C13	1022	βR_1(A1),νC20-C22	1021	νN5-C8νN5-C9
1012m				1007	νN5-C13,ρ'C7-H24		
	1001s	1001	βR_1(A1)	1001	βR_1(A1)	1001	βR_1(A1) νC21-C22
	1001s	995	νC12-O2	998	γC22-H43		
	1001s	992	νN5-C8	995	νC12-O2	989	γC22-H43
981w	982w	989	γC22-H43,γC21-H42	985	νC9-C11	981	νC12-O2
975sh		976	νC9-C11νC8-C10	974	νC8-C10	969	νC8-C10,νC9-C11
		965	$\tau_w CH_2$(C15) νC14-C15	965	γC21-H42γC20-H41	964	$\tau_w CH_2$(C16), νC14-C15 δC14C15C16
958vw	961w	961	γC19-H39,γC20-H41	959	$\tau_w CH_2$(C16)	960	γC20-H41
		950	νC7-C9,νC6-C8	949	νC6-C8,νC7-C9	940	νC7-C9
		942	τR_2(A2)			932	νC12-O2,τR_2(A2)
923sh	920w			925	νN5-C13		
915w	910sh	919	γC18-H38	921	γC19-H39		
906w	906w					915	γC18-H38,γC19-H39
899w	899sh	892	νC7-O1	888	νC7-O1	890	νC7-O1,νC6-C8
874vw	875w	880	νC6-O1	875	νC6-O1	878	νC6-O1
	864vw	867	γCOO	861	γCOO	865	νC6-C7
851s	852w			854	γC18-H38	853	τR_1(A3)
851s	852w	851	γC21-H42			851	γC21-H42
		845	τR_1(A3)				
843sh	841w	841	νC6-C7	839	νC7-O1,τR_1(A3)		
836sh	836sh	827	δCOO	836	νC6-C7	840	νC6-C7
810w	811w	811	$\tau_w CH_2$(C10) $\tau_w CH_2$(C11)	819	$\tau_w CH_2$(C16)νC14-O2	823	νC7-C9
780w	802w			797	$\tau_w CH_2$(C11)	806	βR_2(A3)
776sh		775	τR_1(A1),γC22-H43	774	τR_1(A1),γC22-H43	772	τR_1(A1),γC22-H43
753w	755m	767	τR_1(A2) γN5-C13			751	$\tau_w CH_2$(C11)
				745	γN5-C13,τR_1(A2)	748	βR_1(A3), $\tau_w CH_2$(C10)

	745sh	741	γC22-H43	740	τR_1(A2), βR_1(A3)	738	γCOO
735m		731	βR_2(A3), νN5-C9				
725sh	728w	728	βR_1(A3)	722	βR_1(A3)		
699m	706vw	697	τR_1(A1), τR_2(A1)	699	νN5-C8,νN5-C9	697	τR_1(A1)
694sh				698	τR_1(A1)	688	τR_1(A2),βR_1(A3)
678vw		674	τR_2(A2), βR_3(A2)			681	τR_2(A3)
	666w	666	βR_3(A1)	667	δC12O2C14		
				663	ρCOO	660	βR_3(A1)
	629w	628	βR_2(A1)	628	βR_2(A1)	628	βR_2(A1)
	616w						
	588w	574	βR_3(A1) γCOO	573	βR_3(A1),γCOO	572	γCOO
	554w	546	βR_3(A2)	538	βR_2(A3)	546	βR_2(A2), βR_3(A2)
	534w	534	τR_2(A1)	530	τR_2(A1),γC15-C17	537	τR_2(A1)
	489sh	496	τR_2(A1)			506	τOH
	484w	470	τOH	489	τR_2(A1)	486	τR_2(A1), τR_1(A2)
	461w	463	τR_2(A2)	454	δO2C12C10 δO2C12C11	458	τR_2(A2,)τR_1(A2)
	458sh	450	γN5-C13δCCO1			447	γN5-C13, δCCO
	435w			432	γN5-C13,δCCO1		
		405	τR_3(A1)	404	τR_3(A1)	404	τR_3(A1)
		402	τR_1(A2)	399	δO4C16C15	401	δO4C16C15
	395vw	380	βR_2(A2)	392	τOH		
	367w			367	βR_2(A2)	375	βR_2(A2),βN5-C13
	337sh	336	τR_1(A2)				
	330w	330	δO4C16C15	328	βC15-C17	331	βC15-C17
		319	ρC15-C17	318	τR_1(A2), τR_2(A2)	319	τR_1(A2), τR_2(A2)
	310w			315	τR_2(A2), τR_3(A2)	315	δO2C12C10, δO2C12C11
	292w	302	τR_1(A2), τR_2(A1)	294	τR_1(A2)	297	τR_2(A3)
		286	ρN5-C13,τR_2(A3)	274	τR_1(A3) ,ρN5-C13	288	τR_1(A2)
	269w	275	τR_1(A2),τR_2(A2)	273	τR_2(A3)		
	261w	245	τR_3(A2)			261	τR_2(A2)τR_1(A2)
	234sh	243	δC14C15C16	235	δC14C15C16	233	τR_3(A2)
	219w			231	τR_3(A2)	226	τR_2(A2)
	207w	193	τR_2(A2) βR_3(A2)				
		181	ρCOO	188	βR_3(A2)	185	βR_3(A2)
	175sh			174	$\tau_w CH_3$		
	167w	153	νBr45-H44	166	τR_2(A2)τR_1(A2)	170	ρCOO
	145w	143	τR_2(A2) τR_1(A2)			148	$\tau_w CH_3$
				130	τR_2(A2)τR_1(A2)	133	τR_2(A2)
		120	$\tau_w CH_3$			117	τC16-C15
	109vs	113	τC16-C15	108	τC16-C15		
	89sh	87	δC12O2C14				
	89sh	85	γC15-C17. δC17C15C16	84	γC15-C17 δC17C15C16	81	γC15-C17, δC14C15C17 δC17C15C16
	78sh	59	τR_2(A2), τH44-N5	61	τR_2(A2)		
		51	τO2-C12	56	τR_1(A2)	58	τR_2(A2)τR_1(A2)
		36	τ_wC15-C17			47	τO2-C12
		33	τR_2(A2) τR_1(A2)	35	τ_wC15-C17	32	τ_wC15-C17
				23	τC14-O2	24	τC14-O2
		20	τC14-O2	21	τ_wCOO	20	τ_wCOO
		8	τ_wCOO				

Abbreviations: ν, stretching; β deformation in the plane; γ deformation out of plane; wag, wagging;

τtorsion; β_R, deformation ring τ_R, torsion ring; ρ, rocking; τw, twisting; δ, deformation; a, antisymmetric; s, symmetric; (A_1), Ring 1; (A_2), Ring 2, (A_3), Ring 3. [a]This work, [b]From scaled quantum mechanics force field.

Table S5. Observed and calculated wavenumbers (cm^{-1}) and assignments for R(+) and S(-) forms of Camphor in gas phase by using the B3LYP/6-311++G method.**

Exp[b]		B3LYP/6-311++G** method[a]			
		R(+)		S(-)	
IR	Raman	SQM[c]	Assignments[a]	SQM[c]	Assignments[a]
2961s	2988vs	2988	ν_aCH_3(C10)	2988	ν_aCH_3(C9)
2941sh		2976	ν_aCH_3(C9)	2976	ν_aCH_3(C10)
	2972sh	2969	ν_aCH_2(C6)	2969	ν_aCH_2(C6)
		2968	ν_aCH_3(C11)	2968	ν_aCH_3(C11)
		2964	ν_aCH_3(C11)	2964	ν_aCH_3(C11)
		2961	ν_aCH_2(C7)	2961	ν_aCH_2(C7)
	2953s	2955	ν_aCH_3(C9)	2955	ν_aCH_3(C10)
		2951	ν_aCH_2(C5)	2951	ν_aCH_2(C5)
2948s		2948	νC4-H12	2948	νC4-H12
		2948	ν_aCH_3(C10)	2948	ν_aCH_3(C9)
	2929sh	2930	ν_sCH_2(C6)	2930	ν_sCH_2(C6)
		2927	ν_sCH_2(C7)	2927	ν_sCH_2(C7)
2917sh		2921	ν_sCH_2(C5)	2921	ν_sCH_2(C5)
		2906	ν_sCH_3(C10)	2906	ν_sCH_3(C9)
		2903	ν_sCH_3(C11)	2903	ν_sCH_3(C11)
2877w	2889s	2899	ν_sCH_3(C9)	2899	ν_sCH_3(C10)
1743vs	1751m	1737	νC8=O1	1737	νC8=O1
1471w	1476m	1464	δCH_2(C6)	1464	δCH_2(C6)
1453sh	1452m	1453	δCH_2(C5), δ_aCH_3(C9)	1453	δCH_2(C5), δ_aCH_3(C9)
1445m	1444sh	1449	δ_aCH_3(C9)	1449	δ_aCH_3(C10)
1439sh		1438	δCH_2(C5) δ_aCH_3(C9)	1438	δ_aCH_3(C10)
		1434	δ_aCH_3(C11)	1434	δ_aCH_3(C11)
1422sh		1428	δ_aCH_3(C10)	1428	δ_aCH_3(C11)
		1423	δ_aCH_3(C11)	1423	δ_aCH_3(C11), δ_aCH_3(C11)
1418m	1420m	1420	δ_aCH_3(C10)	1420	δ_aCH_3(C9)
1390m	1392vw	1395	δCH_2(C7)	1395	δCH_2(C7)
1372m	1378vw	1364	δ_sCH_3(C9)	1364	δ_sCH_3(C10)
		1349	δ_sCH_3(C11)	1349	δ_sCH_3(C11)
1332sh	1326w	1343	δ_sCH_3(C10)	1343	δ_sCH_3(C9)
1324m		1313	wagCH_2(C5)	1313	wagCH_2(C5)
1318sh	1204sh	1305	wagCH_2(C6)	1305	wagCH_2(C6)
1280w	1298w	1289	ρ'C4-H12	1289	ρ'C4-H12
1247w	1276vw	1258	ρC4-H12	1258	ρC4-H12
1240sh	1248w	1240	wagCH_2(C7), νC4-C7 ρCH_2(C5)	1240	wagCH_2(C7),νC4-C7 ρCH_2(C5)
1222w	1221w	1233	τR_1(A1)	1233	τR_1(A1)
1197w	1199w	1209	ρCH_2(C6)	1209	ρCH_2(C6)
	1193w	1188	τR_2(A1)	1188	τR_2(A1)
1169w	1169w	1174	τR_3(A3),τR_2(A1)	1174	τR_3(A3),τR_2(A1)
1163sh	1152w	1153	ρCH_2(C7),ρC4-H12 ρCH_3(C11)	1153	τR_2(A3) νC3-C11

1127w	1131vw	1120	τR_2(A1), τR_1(A2)	1120	τR_2(A1), τR_1(A2) $\rho'CH_3$(C11)
1095w	1093w	1109	τR_3(A3), τR_1(A2)	1109	τR_3(A3), τR_1(A2)
1075w	1079w	1087	$\rho'CH_3$(C11)	1087	ρCH_3(C11)
1047s	1047vw	1066	τR_1(A2)	1066	τR_1(A2)
1022m	1022w	1014	τR_1(A2),τR_2(A1)	1014	τR_1(A2), τR_2(A2)
990vw	1011w	997	ρCH_3(C10)	997	$\rho'CH_3$(C9),$\rho'CH_3$(C10)
960sh	986w	982	τR_1(A2),τR_2(A1)	982	τR_1(A2), τR_2(A2)
952w	950m	963	τR_3(A3), τR_1(A2)	963	τR_3(A3), τR_1(A2)
934w	934w	929	$\rho'CH_3$(C9), νC2-C10 $\rho'CH_3$(C10) ρCH_3(C9)	930	ρCH_3(C10), νC2-C9 ρCH_3(C9)
926w	926sh	924	νC2-C9	924	νC2-C10
915w	914w	907	νC5-C6	907	νC5-C6
858sh	862s	888	τR_3(A3), τR_1(A2)	888	τR_3(A3), τR_1(A2)
855w	850s	874	τR_3(A3),τR_2(A1)	874	τR_3(A3), τR_2(A1)
848sh	846sh	831	νC4-C6	831	νC4-C6
829w	822w	822	νC3-C5	822	νC3-C5
751m	772vw	776	τR_2(A3),τwCH_2(C6)	776	τR_2(A3), τwCH_2(C6)
709vw	747w 706w	703	τwCH_2(C5), νC2-C3 νC3-C8	703	τwCH_2(C5), νC2-C3 νC3-C8,τwCH_2(C7)
647w	648vs	678	νC2-C4	678	νC2-C4
610w	604w	622	νC3-C11,νC7-C8 βC8=O1	622	νC3-C11,νC7-C8 βC8=O1
574w	568w	588	τR_2(A1), γC8=O1	588	τR_2(A1), γC8=O1
552w	549s	553	τR_3(A3),τR_2(A1)	553	τR_3(A3),τR_2(A1)
521s	530vw	538	τR_1(A2), τR_1(A1)	538	τR_1(A2), τR_1(A1)
514sh	515w	511	τR_1(A2)	511	τR_1(A2)
472w	468m	464	τR_2(A2)	464	τR_2(A2)
415w	410w	402	τR_1(A3)	402	τR_1(A2),τR_2(A1)
	386w	389	δC10C2C9,δC9C2C3 δC10C2C4 δC9C2C4	389	δC9C2C3,δC10C2C9 δC9C2C4 δC10C2C4
	375sh	373	τR_1(A2)τR_2(A1) δC11C3C5	373	τR_1(A2)τR_2(A1) δC11C3C5
	292w	292	τR_1(A2),τR_3(A3)	292	τR_1(A2),τR_3(A3)
	281w	284	τR_1(A2)	284	τR_3(A3), τR_1(A2)
	254m	256	τR_3(A3)	256	τR_3(A3), τR_1(A2)
	237w	236	τR_1(A2),τR_3(A3) δC11C3C2	236	τR_1(A2),τR_3(A3) δC11C3C2
	210w	209	τR_3(A3), τR_1(A2)	209	τR_3(A3)
	197sh	200	τwCH_3(C9),τwCH_3(C10) τwCH_3(C11)	200	τwCH_3(C10), τwCH_3(C9)
		156	τR_3(A3), τR_1(A2)	156	τR_3(A3), τR_1(A2) τwCH_3(C11)
		150	τR_1(A2),τR_3(A3)	150	τR_1(A2),τR_3(A3)
		106	τR_3(A3),τR_2(A1)	106	τR_3(A3)

Abbreviations: ν, stretching; β, deformation in the plane; γ, deformation out of plane; wag, wagging; τ , torsion; β_R, deformation ring τ_R, torsion ring; ρ, rocking; τw, twisting; δ, deformation; a, antisymmetric; s, symmetric; (A_1), Ring 1; (A_2), Ring 2; (A_3), Ring 3; [a]This work, [b]From Ref [46], [c]From scaled quantum mechanics force field.

[46] Experimental available ATR, IR and Raman spectra of camphor from: https://spectrabase.com/spectrum.

Table S6. Experimental frequencies (cm^{-1}) and assignments for chromyl nitrate

[a]Experimental spectra				[b]Assignment			[a]Assignment
[a]IR	[a]IR	[a]IR	[a]Raman	(monodentate)	(bidentate)	(bidentate)[#]	
1900 vvw	1893 vvw	1910		959 + 945 = 1904			1224 + 685= 1909
1650 sh	1640 sh	1660 sh	1642 (16)	ν_s NO_2 ip	ν N=O ip	ν N=O ip	$\nu_{a\bar{n}}$ N=O
1637 vs	1613 vs	1635 vs	1614 sh	ν_s NO_2 op	ν N=O op	ν N=O op	
1556	1550 w	1550					2 x 778 =1556
		1381					944 + 453 = 1397
		1348					1223 + 125 = 1348
		1337		1234 + 100 = 1334			
	1305 w						958 + 349 = 1307
	1275	1276		1637 – 349= 1288			
1227	1234 sh		1232 (11)	ν_a NO_2 ip	ν_a NO_2 ip	ν_a NO_2 ip	$\nu_{s\bar{n}}$ N=O
1221	1215 s	1223	1216 sh	ν_a NO_2 op	ν_a NO_2 op	ν_a NO_2 op	
		1023					775 + 247 =1022
961		968		835 + 125 = 960			ν_a Cr=O
	958 s	962 sh	959 (100)	ν_s Cr=O	ν_s Cr=O	ν_s Cr=O	ν_s Cr=O
		944	945 sh	ν_a Cr=O	ν_a Cr=O	ν_a Cr=O	ν N-O
		835		δNO_2 ip	δNO_2 ip	ν_s NO_2 ip	γN=O
808 sh	806 sh	800		δNO_2 op	δNO_2 op	ν_s NO_2 op	457 + 349 = 806
781 sh	779 sh	781	782 (8)	γN=O op,	γN=O op,	δNO_2 ip,	δNO_2
776	771 m	774	774 sh	δO=N–O op,	ν_s NO_2 ip,	γN=O ip,	δNO_2
	685 w	689	686 (10)	ν_a N-O, ν_s N-O	δO=N–O op,	δO=N–O op,	ρNO_2
	457 m	453	460 sh	ν_a Cr-O	δCrO_2	δCrO_2	ν_a Cr-O
			446 (95)	δCrO_2	ν_a Cr-O	ν_s Cr←O	ν_s Cr-O
	349 w		350 (41)	ν_s Cr-O	ν_s Cr-O	ν_s Cr-O	δCrO_2
	273 w		271 (9)	Wag CrO_2	τNO_2 op	Wag CrO_2	ρ CrO_2
	247 w		242 (5)	τNO_2 ip	ρ CrO_2	ρ CrO_2	δN-O-Cr
	223 sh			δN-O-Cr op	Wag CrO_2	τw CrO_2	

213 w					
	206 (9)	δN-O-Cr ip,	ν_a Cr←O	ν_a Cr-O,	
	152 (5)	ρ CrO_2 ,	δa O-Cr-O	δa O-Cr-O,	τNO_2
125 br, vw	100	τNO_2 op,	τN=O,	τNO_2 ip,	
-	-		τNO_2 ip	τNO_2 op	

Abbreviations: □, stretching; □, deformation; □, rocking; wag, (□) wagging; □w, torsion, a, antisymmetric, s, symmetric, op, out of phase; ip, in phase

[a]Ref [1] E. L. Varetti, S. A. Brandán, A. Ben Altabef, *Vib. Spectrosc*.**1993**, *5*, 219, [#]Considering the nitrate group as ring of four members.

[b]Ref [60]

Table S7. Comparison of scaled internal force constants for chromyl nitrate

Force Constants	[a]CHROMYL NITRATE								
	MONODENTATE			BIDENTATE			[#]BIDENTATE		
Coordinates	Lanl2DZ	6-31G*	6-311++G	Lanl2DZ	6-31G*	6-311++G	Lanl2DZ	6-31G*	6-311++G
f (N=O)	16.18	16.25	15.83	11.74	11.44	11.71	11.55	11.62	11.07
f (N-O)	3.19	3.38	3.22	4.62	4.96	4.62	4.96	4.96	4.62
f (Cr=O)	6.55	6.55	6.56	6.55	6.53	6.57	6.55	6.57	6.56
f (Cr-O)	7.82	6.09	7.34	1.64	1.44	1.51	1.34	1.38	1.27
f (O=N=O)	1.57	1.62	1.58	-	-	-	-	-	-
f (O=N-O)	2.05	2.24	2.09	1.83	1.74	1.87	1.49	1.32	1.57
f (O=Cr=O)	2.31	2.53	2.26	1.73	1.66	1.74	1.58	1.62	1.63
f (O-Cr-O)	0.86	0.80	0.74	0.91	0.93	0.93	0.75	0.65	0.66
f (O-N-Cr)	1.96	2.41	1.96	-	-	-	-	-	-
f (N=O)/ (N-O)	1.74	1.81	1.71	1.33	1.29	1.25	1.66	1.95	1.60
f (N=O)/ (Cr-O)	1.16	1.16	1.16	-0.12	-0.07	-0.11	-0.27	-0.47	-0.39
f (N-O)/ (N-O)	2.00	2.06	2.09	-1.30	-1.29	-1.29	-1.35	-1.61	-1.36

Units are mdyn $Å^{-1}$ for stretching and stretching/stretching interaction and mdyn Å rad^{-2} for angle deformations

[a]Ref [60], [#]Considering the nitrate groups as ring of four members

Table S8. Observed and calculated frequencies (cm^{-1}) for niobyl nitrate

Niobyl nitrate[a]					
IR Solid			Raman	Assignment	Assignment
CsI	KBr	Polyethylene	solid	(Two nitrate bidentate)	(Three nitrate bidentate)
1763 w	1765 w			ν(N=O) ip	ν(N=O)ip
1753 w				ν(N=O) op	ν(N=O)op
1620 s	1614 m		1605 w	νa(NO_2)*	ν(N=O)*
1398 vs				νs(NO_2)*	
1379 vs	1389 vs				νa(NO_2)*
1362 vs				νa(NO_2) ip	νa(NO_2) ip
1345 vs	1344 sh			νa(NO_2) op	νa(NO_2) op
			1303 w	652 x 2 = 1304	652 x 2 = 1304
1264 w			1267 vw	671 + 582 = 1253	671 + 582 = 1253
1050 w			1057 m	ν(Nb=O)	ν(Nb=O)
	986 sh		1035 sh		
947 sh			954 sh	νs(NO_2) ip	νs(NO_2) ip
930 sh				νs(NO_2) op	νs(NO_2) op
920 w	910 s			ν(N-O)*	νs(NO_2)*
905 w				δ(NO_2) ip	δ(NO_2) ip
888				γNO_2*	γN=O*
870			864 sh	γN=O ip	γN=Oip
812	818 vs			γN=O op	γN=O op
797	795 vs			δ(NO_2) op	δ(NO_2) op
737			728 s	δ(O=N-O)*	δ(O=N-O)*
726			707 s	δ(O=N-O) ip	δ(O=N-O) ip
668	671 s	668 w	688 s	δ(O=N-O) op	δ(NO_2)*
618			652 s	δ(NO_2)*	δ(O=N-O) op
588	582 s		582 sh		
		563 s			
496		495 w		ν(Nb-O-Nb)	ν(Nb-O-Nb)
451		457 sh	456 w		
435		442 sh	438 vw		
421		419 w		ν(Nb-O)	ν(Nb-O)
406		398 w		νa(Nb-O)*	ν(Nb-O)
355	349 m	351 s	342 sh	ν(Nb-O)	νa(Nb-O)*
	295 w	302 sh		νs(Nb-O)*	νs(Nb-O)
		289 sh	271 sh	ν(Nb-O)	ν(Nb-O)
	248 s	265 vs		δ(N-O-Nb)	δ(NbO_2), δ(O=Nb-O)
	212 s	228 s	226 s	δ(O=Nb-O)	νs(Nb-O)*, ρ(O=Nb-O)
	205 m	202 m	206 s	δ(NbO_2)	δ(NbO_2)
		178 m		ρ(O=Nb-O)	
		157 w		δ(NbO_2)	τ(NO_2)*
		150 w		δ(NbO_2)	
		140 w		τ(NO_2) op	τ(NO_2) op
		121 w		δ(NbO_2)	δ(NbO_2)

	109 vs	$\tau(NO_2)$*	
89 w	90 vs	δ(O=Nb-O)	$\delta(NbO_2)$, δ(O=Nb-O)
72 w		$\tau(NO_2)$ip	$\tau(NO_2)$ip
		$\tau(NO_3)$*	$\tau(NO_3)$*

Abbreviations: ν, stretching; δ, deformation; ρ, rocking; wag, (γ) wagging; τw, torsion, a, antisymmetric, s, symmetric; op, out-of-phase; ip, in-phase; s, strong; v, very; m, medium; w, weak; sh, shoulder. [a]Ref [62], *single nitrate group lies in the mirror plane.

Table S9. Comparison of scaled internal force constants for niobyl nitrate with the corresponding to vanadyl nitrate

	B3LYP/6-31G*			
Force constants	ONE NITRATE MONODENTATE		THREE NITRATE	
Coordinates	[a]$NbO(NO_3)_3$	[b]$VO(NO_3)_3$	[a]$NbO(NO_3)_3$	[b]$VO(NO_3)_3$
f (N=O)	12.07	11.42	12.07	11.29
f (N=O)*	8.65	9.20	11.69	11.03
f (N-O)	5.03	6.07	4.14	6.08
f (N-O)*	4.28	5.12	4.12	6.18
f (M=O)	7.49	7.39	7.49	7.39
f (M-O)	1.51	1.57	1.51	1.57
f(M-O)*	2.47	2.51	1.46	1.45
f (O-N-O)	1.89	1.76	1.89	1.76
f (O-N-O)*	1.76	1.60	1.65	1.73
f (O=N-O)	1.34	1.20	1.34	1.20
f (O=M-O)	0.89	1.15	0.96	1.15
f (O-M-O)	0.83	0.75	0.78	0.75

Units are mdyn $Å^{-1}$ for stretching and stretching/stretching interaction and mdyn Å rad^{-2} for angle deformations. [a]Ref [62], [b]Ref [61]. *A single nitrate group lies in the mirror plane M= Nb, V

Table S10. Observed and calculated wavenumbers (cm^{-1}) and assignments for 4PPHP in gas phase.

Experimental	B3LYP/6-311++G** Method[a]		
IR[c]	Calculated	SQM[b]	Assignments[a]
3567vs,br	3841	3682	νO29-H30
3567vs,br	3838	3680	νO31-H32
3567vs,br	3497	3353	$\nu_s NH_2 \nu_a NH_2$
3263sh	3204	3071	νC14-H15
	3191	3059	νC18-H19
	3182	3050	νC22-H23
3167sh	3168	3037	νC16-H17
	3162	3031	νC20-H21
	3121	2992	$\nu_a CH_2$(C7)
3107sh	3090	2963	$\nu_a CH_2$(C4)
	3083	2956	$\nu_a CH_2$(C10)
	3082	2955	$\nu_a CH_2$(C1)
	2997	2873	$\nu_s CH_2$(C1)
2992sh	2993	2870	$\nu_s CH_2$(C10)
	2952	2830	$\nu_s CH_2$(C7)
2883w	2945	2823	$\nu_s CH_2$(C4)

2493vs,br	2396	2298	νO33-H26
1640m	1640	1587	νC20-C22,νC14-C16
1600s	1615	1564	νC13-C14
1504s	1528	1482	βC20-H21
1451s	1509	1459	wagNH_2 ρNH_2
	1502	1445	δCH_2(C1),δCH_2(C10)
	1495	1440	βC18-H19,βC16-H17
1438sh	1491	1438	δCH_2(C7)
1431sh	1487	1429	δCH_2(C4)
1428sh	1481	1425	δCH_2(C1), δCH_2(C10)
1395w	1430	1400	wagCH_2(C4), wagCH_2(C7)
	1414	1390	wagCH_2(C4), wagCH_2(C10)
	1408	1361	τO33-H26,τN24-H26
1349sh	1381	1357	wagCH_2(C7)
1331sh	1369	1332	wagCH_2(C1)
	1363	1330	ρCH_2(C4)
1325m	1354	1324	βC22-H23
1260vs	1328	1284	νC13-C22
1260vs	1323	1280	ρCH_2(C1)
1260vs	1289	1238	$\nu_a PO_2$
1233sh	1269	1234	ρCH_2(C10)
1233sh	1257	1220	νC13-N27
1197sh	1234	1199	ρCH_2(C7)
	1209	1175	βC16-H17,βC14-H15
1154s	1182	1150	βC18-H19
1154s	1169	1127	νN27-C4,νN27-C7
	1166	1118	τO33-H26,τN24-H26
1091vs	1142	1070	νC14-C16
	1107	1059	τO33-H26,τN24-H26
1041s	1104	1043	τO33-H26,τN24-H26
	1076	1030	βR_1(A1), βR_1(A2)
1025sh	1068	1023	τwCH_2(C10)
1018sh	1060	1014	νC18-C20,νC16-C18
991m	1057	1004	δO29-H30
991m	1051	990	βR_1(A1)
	1025	982	γC18-H19
969sh	1008	969	δO31-H32
	991	967	τO33-H26,τN24-H26
959vs	973	963	γC16-H17,γC20-H21
919vs	967	924	$\nu_s PO_2$
	950	906	νN27-C7,νN24-C10
	935	902	γC14-H15,γC22-H23
879s	907	880	γC14-H15
856m	896	854	τwNH_2,νC1-C4,νC7-C10
	864	825	γC22-H23
856m	850	817	$\nu_a PO_2$H

	849	805	νC1-N24,νN24-C10
764vs	830	784	τwCH_2(C7),τwCH_2(C1)
	788	759	τR_1(A1),γC18-H19
764vs	772	757	$\nu_s PO_2H$
723sh	745	720	βR_2(A1)
690s	707	688	τR_1(A1)
631w	642	627	βR_3(A1)
585sh	632	618	βR_1(A2)
549sh	554	543	βR_2(A2)
519sh	533	522	τR_3(A1), γC13-N27
	477	469	βR_3(A2)
512vs	471	468	τwPO_2H
512vs	468	462	$\nu_a NH_2$,$\nu_s NH_2$
	439	434	$wagPO_2H$
	436	430	βC13-N27,βN27-C13
410sh	418	405	τR_2(A1)
	414	401	τR_1(A2)
	391	375	$\delta_a PO_2H$, $\delta_a PO_2$
	365	353	ρPO_2H
	320	311	τR_3(A2)
	309	303	βR_2(A2), νC13-N27
	269	261	τR_2(A2)
	257	247	$\nu_a NH_2$,$\nu_s NH_2$
	250	231	τO29-H30,τO31-H32
	197	185	$\nu_a NH_2$,$\nu_s NH_2$
	184	178	$\delta_a PO_2H$
	136	133	$\nu_s NH_2$,$\nu_a NH_2$
	82	80	δN24H26O33, δP28O33H26
	74	71	$\nu_s NH_2$,$\nu_a NH_2$
	62	58	τO33-H26
	45	41	τ_wN27-C13,τP28-O33
	23	21	τN24-H26,τO33-H26
	19	17	δNH_2
	15	14	τN24-H26

Abbreviations: ν, stretching; δ, deformation in the plane; γ, deformation out of plane; wag. wagging; τ, torsion; β_R. deformation ring τ_R. torsion ring; ρ. rocking; τw. twisting; δ. deformation; a. antisymmetric; s. symmetric; (A_1), Ring Phenyl; (A2), Ring piperazine; [a]From Ref [70], [b]From scaled quantum mechanics force field.

Table S11. Observed and calculated wavenumbers (cm^{-1}) and assignments of anhydrous, mono and dihydrated chloride salts in the gas phase by using the hybrid B3LYP/6-311++G level of theory.**

Experimental[c]		B3LYP/6-311++G** Method[a]					
		Anhydrous Salt		Monohydrated Salt		Dihydrated Salt	
IR	Raman	SQM[b]	Assignments	SQM[b]	Assignments	SQM[b]	Assignments
3430w						3723	ν_aO50-H51
3372w				3714	ν_aO46-H47	3716	ν_aO46-H47
3154vw	3173w			3087	νC36-H41	3290	ν_sO50-H51νCl49-H51

	3145w	3098	νC36-H41	3073	ν_sO46-H47	3178	ν_sO46-H47νCl49-H48
3089sh		3090	νC18-H23	3069	νC29-H34	3082	νC36-H41
		3069	νC29-H34	3068	νC37-H42	3069	νC25-H30
		3068	νC3-H8	3066	νC17-H22	3068	νC38-H43
		3065	νC37-H42	3066	νC3-H8	3066	νC3-H8
		3064	νC17-H22	3062	νC26-H31	3062	νC28-H33
	3068s	3061	νC26-H31	3060	νC39-H44	3061	νC39-H44νC37-H42
3056w		3058	νC39-H44	3059	νC6-H11	3059	νC6-H11
		3057	νC6-H11	3054	νC28-H33	3055	νC15-H20νC16-H21
		3056	νC15-H20	3054	νC15-H20	3054	νC26-H31
		3053	νC28-H33	3050	νC38-H43	3051	νC4-H9
		3048	νC4-H9	3049	νC4-H9	3050	νC38-H43νC40-H45
		3047	νC40-H45	3046	νC25-H30	3047	νC29-H34
		3046	νC25-H30			3044	νC16-H21νC17-H22
		3043	νC16-H21	3041	νC40-H45	3042	νC40-H45
				3040	νC16-H21	3039	νC27-H32
	3040sh	3038	νC27-H32	3039	νC27-H32	3038	νC5-H10
		3036	νC38-H43	3037	νC5-H10	3037	νC17-H22
2968s		3035	νC5-H10	3031	νC14-H19	3032	νC14-H19
2936vs	2955w	3034	νC14-H19	2995	νC18-H23	3028	νC18-H23
2863s	2886w	2875	νC7-H12	2985	νC7-H12	2992	νC7-H12
						2123	βC7-H12
1589m	1596vs	1575	νC25-C26,νC28-C29	1584	δW1	1575	δW2,νC28-C29
	1585sh	1573	νC14-C15	1575	νC25-C26,νC28-C29	1575	νC39-C40,νC36-C37
		1572	νC6-C7,νC3-C4	1575	νC39-C40	1575	δW2
		1571	νC39-C40,νC36-C37	1573	τwH12-C7,τwW1	1573	βC7-H12,δW1
				1569	νC14-C15,νC17-C18	1569	δW2,τwW2
		1562	νC27-C28	1565	νC38-C39,νC37-C38	1566	βC7-H12,τwH12-C7
		1559	νC15-C16,νC16-C17	1561	τwH12-C7, νC5-C6	1563	βC7-H12,τwH12-C7
		1558	νC38-C39	1560	νC27-C28,νC26-C27	1561	νC26-C27,νC27-C28
		1556	νC5-C6,νC4-C5	1556	νC15-C16,νC16-C17	1556	νC15-C16,νC18-C13, νC16-C17,νC17-C18
	1492w	1478	βC7-H12,βC4-H9	1483	βC7-H12	1520	βC7-H12,τwH12-C7
		1472	βC28-H33,βC26-H31	1472	βC40-H45,βC36-H41	1476	βC17-H22
1474s		1470	βC39-H44	1471	βC25-H30,βC29-H34	1472	νC35-C36,νC38-C39
1448s	1447w	1469	βC14-H19,βC18-H23	1467	βC14-H19	1471	βC29-H34,βC25-H30
		1427	βC27-H32	1429	βC38-H43,βC39-H44	1430	τwH22-C17,τwW2
		1423	βC16-H21,βC15-H20	1424	βC27-H32, βC38-H43	1426	τwH22-C17,τwW2
		1421	βC27-H32	1422	βC6-H11, νC3-C4	1423	τwH22-C17,τwW2
1386m	1407w	1420	βC5-H10,βC6-H11	1419	βC16-H21,βC17-H22	1422	βP1-C2
1349w	1350w	1341	βC7-H12,βC3-H8	1343	τwH12-C7,τwW1	1407	τwH22-C17,τwH12-C7
1325w	1326w	1326	βC36-H41,βC40-H45	1326	βC36-H41,βC40-H45	1328	βC18-H23,βC14-H19
		1323	βC29-H34,βC25-H30	1324	βC18-H23	1325	βC36-H41,βC40-H45
		1321	βC18-H23,βC14-H19	1321	βC29-H34,βC25-H30	1321	βC25-H30,βC29-H34
1287vw	1297w	1277	νC35-C36	1280	νC35-C36,νC35-C40	1280	βP1-C2,τwW2
		1275	νC18-C13,νC13-C14	1274	νC18-C13,νC13-C14	1277	τwH22-C17,τwW2

		1267	νC2-C7,νC2-C3	1267	νC2-C7,νC2-C3	1269	βP1-C2,βC7-H12
	1245w	1265	νC24-C29,νC24-C25	1266	νC24-C29	1266	νC24-C25,νC24-C29
1190w	1197m	1189	βC6-H11	1192	τwH12-C7,τwW1	1243	τwH22-C17,τwW2
	1177m	1183	βC37-H42	1183	βC37-H42,βC36-H41	1200	τwW2,δC17H22O50
		1180	βC28-H33,βC26-H31	1180	βC17-H22	1181	βC37-H42
		1178	βC17-H22	1178	βC28-H33,βC26-H31	1179	βC26-H31
	1168sh	1155	βC16-H21,βC15-H20	1159	βC38-H43,βC39-H44, βC37-H42	1160	βC15-H20
1164w	1164sh	1155	βC38-H43	1155	βC27-H32,βC26-H31, βC28-H33	1159	βC38-H43,βC39-H44
		1154	βC5-H10,βC4-H9	1155	βC5-H10,βC4-H9	1158	βC4-H9
		1154	βC27-H32	1153	βC16-H21,βC15-H20	1155	βC27-H32,βC28-H33
				1085	τwH12-C7,τwW1	1127	τwH22-C17
1117s	1086w	1082	νP1-C24	1082	νP1-C24,νC24-C25	1081	νP1-C35,νC13-C14, νP1-C13,βR$_1$(A2)
1103sh	1080w	1080	βR$_1$(A2),νP1-C13	1081	βR$_1$(A2),νP1-C13	1081	νP1-C24
1084w		1079	βR$_1$(A1)	1078	νC36-C37	1078	τwH22-C17
		1076	βR$_1$(A2)	1075	νP1-C35	1076	τwH22-C17,τwW2
		1072	νC17-C18	1072	νC6-C7,βC3-H8	1074	τwH22-C17,τwW2
		1071	βR$_1$(A4), νP1-C35	1071	βR$_1$(A2)	1073	τwH22-C17,τwW2
		1069	νC28-C29	1070	νC28-C29νC25-C26	1070	νC25-C26,νC28-C29
	1054sh	1068	βR$_1$(A1), νP1-C2	1041	γC7-H12	1064	τwH22-C17,τwW2
1033w	1041s	1059	γC7-H12,τR$_1$(A1)	1027	γC17-H22,γC18-H23	1044	τwH22-C17,τwW2
		1021	βR$_1$(A3)	1021	βR$_1$(A4)	1021	τwH22-C17,τwW2
		1019	βR$_1$(A4), νC38-C39	1020	βR$_1$(A3)	1020	βR$_1$(A3), βR$_1$(A4),νC37-C38
		1019	βR$_1$(A2)	1017	βR$_1$(A1)	1018	τwH22-C17,δC36H41O46
	1016vs	1017	βR$_1$(A1),νC4-C5,νC5-C6	1009	γC27-H32,γC28-H33	1016	τwH22-C17,τwW2
		1009	γC27-H32	1005	γC16-H21	1009	γC27-H32,τR$_2$(A3)
		999	γC16-H21	1000	γC4-H9,γC5-H10	1001	γC38-H43,γC37-H42
		999	γC38-H43	1000	γC38-H43,γC37-H42	1001	γC4-H9,γC5-H10
1004m	999sh	999	γC5-H10,γC4-H9	992	γC26-H31	993	τwH22-C17,τwW2
		992	γC26-H31	991	βR$_1$(A4)	991	τwH22-C17,τwW2
		989	νC26-C27	989	νC26-C27,νC27-C28	990	τwH22-C17,τR$_2$(A2)
		988	νC38-C39,νC37-C38	989	γC15-H20	989	βR$_1$(A3) νC27-C28
		988	βR$_1$(A2), νC15-C16	987	νC5-C6,νC4-C5	987	βR$_1$(A1), νC3-C4,νC4-C5, νC5-C6,
		984	βR$_1$(A1),νC5-C6	984	βR$_1$(A2), γC15-H20	986	τwH22-C17,τwW2
		968	γC15-H20,γC17-H22	972	γC39-H44,γC37-H42	974	γC39-H44,γC37-H42
		966	γC40-H45,γC37-H42	954	γC3-H8	957	γC7-H12,γC3-H8,τR$_3$(A1)
946vw	950w	955	γC3-H8	942	γC14-H19,γC25-H30	942	γC14-H19,γC16-H21,γC18-H23
		941	γC25-H30,γC29-H34	938	γC29-H34	939	τwW2,τwH22-C17
		917	γC14-H19	923	γC40-H45, γC36-H41,γC38-H43	925	γC40-H45,γC38-H43
		910	γC36-H41,γC40-H45	868	γC6-H11	893	τwH22-C17,τwW2
867w	876w	868	γC6-H11	856	γC25-H30	867	τwH22-C17,τwW2
		856	γC28-H33	852	γC14-H19	855	γC29-H34,γC26-H31,γC28-H33, γC25-H30
		829	γC18-H23	831	γC36-H41,γC40-H45	833	γC36-H41

789m		818	γC36-H41,γC39-H44	764	δO46H48Cl49	774	τwH22-C17,τwW2
777m	776w	755	τR_1(A1), γC5-H10	756	τR_1(A1), γC7-H12	755	γP1-C2
764m		751	τR_1(A3)	751	τR_1(A3),γC27-H32	751	τR_1(A3),γC27-H32
735s	742w	738	τR_1(A4), τR_1(A2)	748	τR_1(A2), γC16-H21	738	τwH22-C17,τwW2
		736	τR_1(A2),τR_1(A4)	735	τR_1(A4),γC38-H43	728	τwH22-C17,τwW2
		717	βR_3(A4), βR_3(A2)	717	βR_3(A4),νP1-C35	717	τwH22-C17,τwW2
		713	βR_2(A1)	714	βR_2(A1), νP1-C2	714	βR_2(A1), νP1-C2
		709	βR_3(A3)	712	βR_3(A3)	708	τwH22-C17,τwW2
700s	696m	690	τR_1(A3)	693	τR_1(A1)	693	τR_1(A1), τR_2(A1)
	686sh	688	τR_1(A1)	688	τR_1(A3)	687	τR_1(A3)
				683	τR_1(A2), γP1-C13	684	τR_2(A2), γC17-H22,τR_1(A2)
		680	βR_2(A1) βR_3(A4)	681	βR_2(A1), βR_3(A3)	681	τwH22-C17,τR_2(A2)
		675	τR_1(A2)	670	τR_1(A4)	673	τR_1(A4)
		672	τR_1(A4)			654	τH51-O50
626w	631w	627	βR_2(A3)	627	βR_2(A3)	629	τH51-O50,βR_3(A1)
	625sh	625	βR_3(A1)	625	βR_3(A1)	626	βR_3(A1), βR_2(A3)
		624	βR_2(A4), βR_2(A2)	624	βR_2(A4), βR_3(A4)	625	βR_2(A4), βR_3(A4)
		623	βR_2(A4), βR_3(A1)	622	βR_2(A2), βR_3(A2)	622	βR_2(A2), βR_3(A2)
555sh	547w	536	δC24P1C35	537	δC13P1C2	561	τH51-O50,τwW2
537s		521	ρC13P1C2	525	ρC13P1C2	536	δC13P1C2
523sh		516	τ_wC13P1C2	515	τ_wC13P1C2	515	τ_wC13P1C2,τwP1-C2
470w	481w	469	τR_2(A3)	469	τR_3(A1)	470	τwH22-C17,τwW2
				446	τR_2(A3)	453	τO46-H48
444w	453w	447	τR_3(A1),τR_2(A3)	436	ρW1,τO46-H48	443	ρW1,τO46-H48
		433	τR_2(A4)	431	ρW1,τO46-H48	432	τwH22-C17,τwW2
415w	413w	428	τR_2(A2)	426	τR_2(A4), γP1-C35	426	τR_2(A4)
		398	τR_3(A3)			402	τR_3(A2), τwH22-C17
		394	τR_2(A1)	398	τR_2(A1)	395	τR_3(A2),τwW2
		389	τR_3(A4)	393	τR_3(A3)	393	τR_3(A2)
		385	τR_3(A2)	391	τR_3(A2),τR_2(A2)	385	τwW2
				377	τR_3(A4)	379	τR_3(A4)
	296m	283	wagC13P1C2	286	βP1-C2, wagC13P1C2, βP1-C13	288	βP1-C2
	273s	266	δC24P1C35,βP1-C2	266	δC24P1C35	267	βP1-C2
		253	βP1-C2,ρC13P1C2	255	τwH12-C7,τwW1	260	τwW2,τwH22-C17
		246	νP1-C2	246	βP1-C24	249	τwW2
	237sh	238	τR_3(A1)	237	τR_3(A1), τwW1	237	τwH12-C7
	231m	235	νP1-C13,νP1-C35	235	νP1-C13	234	τR_2(A2),τwW2
	215s			217	νCl49-H48	208	WagW2,νCl49-H48
	205sh	195	βP1-C2,βP1-C35	192	τwH12-C7,βP1-C2	207	τwW2,WagW2
		191	βP1-C24	189	γP1-C2,βP1-C35	189	τwP1-C13
		183	βP1-C13,γP1-C2	184	WagW1,τwW1	185	ρW2
						179	WagW2,τwW2
				170	WagW1	174	WagW2
	146w					153	ρW1, WagW1
		122	νH12-Cl46	111	νO46-H12	111	τwH22-C17,τwW2

91	δC7H12Cl46	100	ρW1,τwW1	82	τwH22-C17,τwW2
75	τH12-Cl46,τwP1-C13	72	τwH12-C7,τwW1	73	τwH22-C17,τwW2
		71	δC7H12O46,τwH12-C7	70	τwH12-C7, τwH22-C17
68	γP1-C24	65	δC7H12O46, WagW1	65	τwH22-C17,τwW2
63	τH12-Cl46	63	γP1-C24	63	τwH22-C17,τwW2
60	τwP1-C2, δC24P1C35	56	τwH12-C7,τwW1	59	τwW2,τwH22-C17
55	τwP1-C2,δC7H12Cl46	52	δC7H12O46, ρW1	54	τwH22-C17, WagW2
50	δC13P1C2,γP1-C13	47	δC7H12O46,τwP1-C2	51	τwH22-C17,τwW2
40	τwP1-C,2τwP1-C24	42	τwH12-C7,ρW1	48	δC36H41O46
36	τwP1-C2,δC7H12Cl46	36	τwP1-C13,τwP1-C24, τwP1-C35	35	τwH22-C17,τwW2
		33	τwH12-C7	29	τwH22-C17,τwW2
				27	τwW1,δH48Cl49H51
		24	τwH12-C7,τwW1	26	τwW2,WagW2
22	τwP1-C13			22	τwH12-C7
19	τwP1-C35,τH12-Cl46	17	τwW1	17	τwW2,τwH22-C17

Abbreviations: ν, stretching; β, deformation in the plane; γ, deformation out of plane; wag, wagging; τ, torsion; ρ, rocking; τw, twisting; δ, deformation; a, antisymmetric; s, symmetric; A1, A2, A3 and A4, Ph rings; [a]From Ref [74], [b]From SQMFF/B3LYP/6-311++G** method, [c]From available from Web page: https://www.chemicalbook.com.

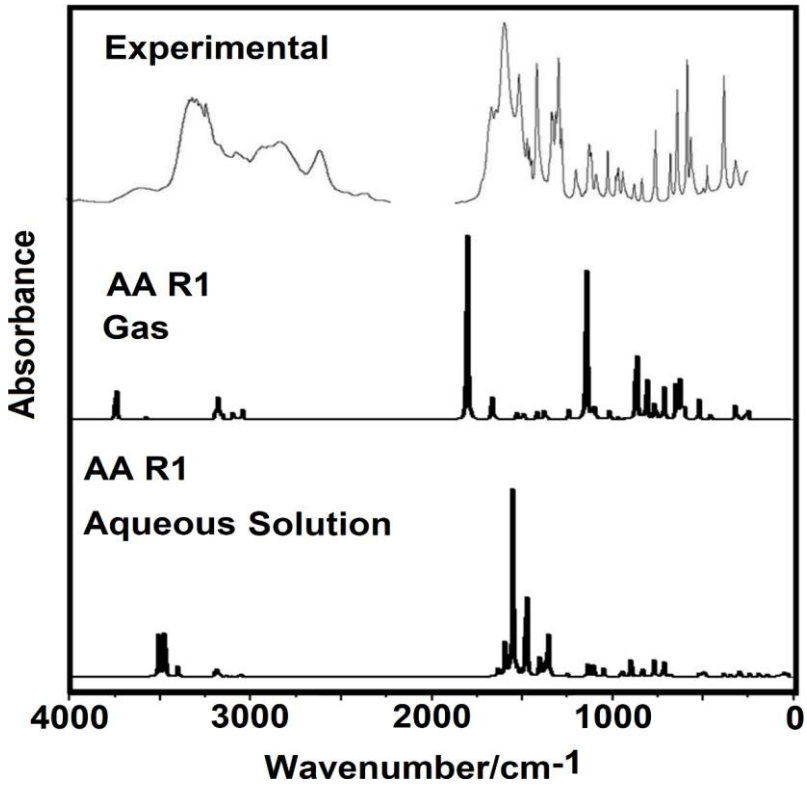

Fig. S1 Comparison of experimental IR spectrum of R1 with the corresponding predicted in gas phase and aqueous solution by using B3LYP/6-311++G calculations**

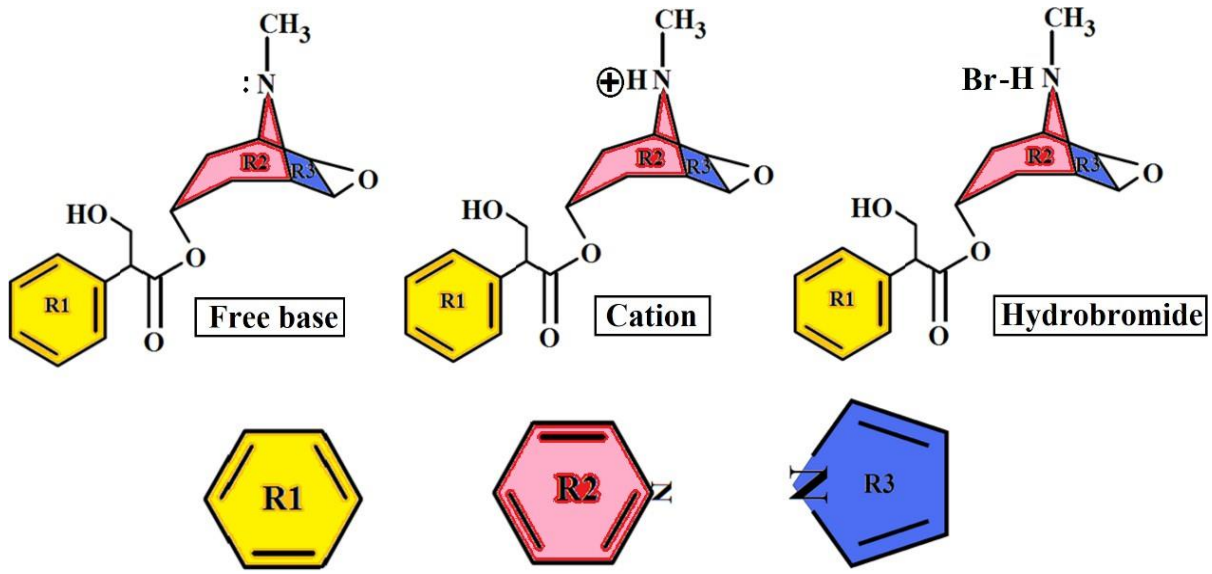

Fig. S2 Molecular structures of free base, cationic and hydrobromide forms of scopolamine showing the quaternary N atom with the N-H⁺···Br⁻ bond and the N-CH3 group presents in all alkaloids. The rings are differenced by diverse colours.

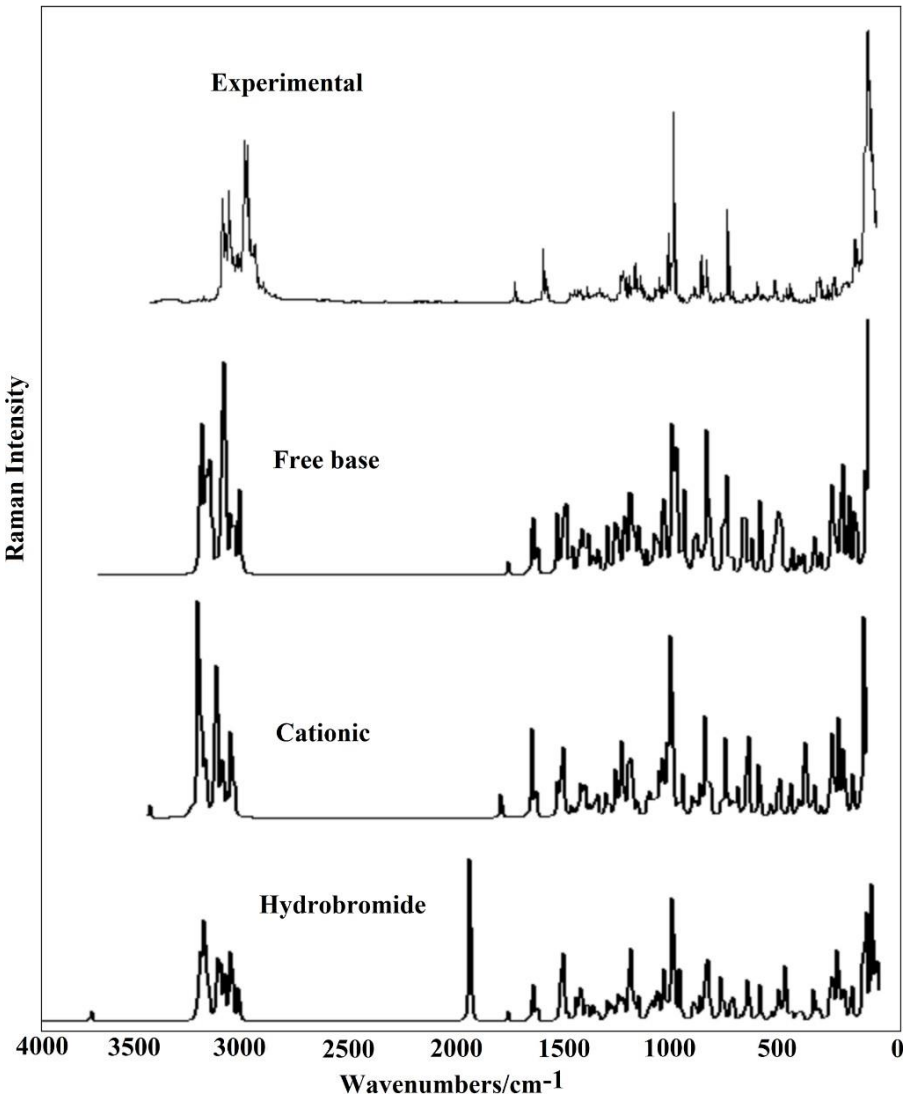

Fig. S3 Comparisons between the experimental FTIR spectrum of hydrobromide of scopolamine in the solid state as tri-hydrate with the corresponding predicted for the free base, cationic and hydrobromide species in gas phase at B3LYP/6-31G level of theory.**